Functional biodiversity and plasticity of methanogenic biomass from a full-scale mesophilic anaerobic digester treating nitrogen-rich agricultural wastes

J.Ruiz-Sánchez[1a], M. Guivernau[1a], B. Fernández[1], J. Vila[1, 2], M. Viñas[1], V. Riau[1], F.X. Prenafeta-Boldú[1,*]

[1] GIRO, Institute of Agrifood Research and Technology (IRTA), Torre Marimon, E08140 Caldes de Montbui, Barcelona, Catalonia, Spain.

[2] Department of Microbiology, University of Barcelona, UB. Av. Diagonal, 643, E08028, Barcelona, Catalonia, Spain.

*Corresponding author: francesc.prenafeta@irta.cat

[a]Both authors contributed equally to this manuscript.

Abstract

The effect of ammonia on methanogenic biomass from a full-scale agricultural digester treating nitrogen-rich materials was characterized in batch activity assays subjected to increasing concentrations of total ammonia N. Acetotrophic and methanogenic profiles displayed prolonged lag phases and reduced specific activity rates at 6.0 gN-TAN L^{-1}, though identical methane yields were ultimately reached. These results agreed with the expression levels of selected genes from bacteria and methanogenic archaea (qPCR of *16S* rRNA and *mrc*A cDNA transcripts). Compound-specific isotope analysis of biogas indicated that ammonia exposure was associated to a transition in methanogenic activity from acetotrophy at 1.0 gN-TAN L^{-1} to intermediate and complete hydrogenotrophy at 3.5 and 6.0 gN-TAN L^{-1}. Such pattern matched the results of 16S-Illumina sequencing of genes and transcripts in that predominant methanogens shifted, along with increasing ammonia, from the obligate acetotroph *Methanosaeta* to the hydrogenotrophic *Methanoculleus* and the poorly understood methylotrophic *Methanomassiliicoccus*. The underlying bacterial community structure remained rather stable but, at 6.0 gN-TAN L^{-1}, the expression level increased considerably for a number of ribotypes that are related to potentially syntrophic genera (e.g. *Clostridium*, *Bellilinea*, *Longilinea*, and *Bacteroides*). The predominance of hydrogenotrophy at high ammonia levels clearly points to the occurrence of the syntrophic acetate oxidation (SAO), but known SAO bacteria were only found in very low numbers. The potential role of the identified bacterial and archaeal taxa with a view on SAO and on stability of the anaerobic digestion process under ammonia stress has been discussed.

Keywords: Ammonia; anaerobic-digestion; active microbiome; C-isotopic biogas fractionation; syntrophic-acetate-oxidation (SAO).

INTRODUCTION

The anaerobic digestion (AD) of organic materials is a well-consolidated technology for the treatment and revalorization of organic waste into renewable energy (methane from biogas), and contributes significantly to the sustainability of several industrial processes (Lettinga, 2010). However, a significant proportion of the organic waste generated by the agrifood sector contains relatively large amounts of nitrogenated compounds (i.e. animal dejections, slaughterhouse by-products, and other protein-rich food-processing wastes). Organic nitrogen compounds are reduced to free ammonia (NH_3), often referred as free ammonia N (FAN), and its ionized counterpart ammonium (NH_4^+). In aqueous media, these two chemical species are in a pH and temperature-depending equilibrium. NH_3 is by far a stronger inhibitor of methanogenesis than NH_4^+ but, because of practical reasons, NH_3 and NH_4^+ are commonly measured together as total ammonia N (TAN) (Yenigün and Demirel, 2013). Such inhibitory effects might affect all microbial communities involved in the AD syntrophy, but the methanogenic archaea appear to be particularly sensitive to ammonia exposure (Demirel and Scherer, 2008). Yet, not all methanogens are affected equally; acetoclastic methanogenic archaea (AMA), which under common non-inhibitory conditions are responsible for most of the generated methane (CH_4), have been described to be vulnerable to relatively low concentrations of ammonia (circa 3.5 gN-TAN L^{-1}) (Banks et al., 2012; Schnürer and Nordberg, 2008). Conversely, the less sensitive hydrogenotrophic methanogenic archaea (HMA) are able to remain active at those concentrations, while reported ammonia inhibition thresholds are above 5 gN-TAN L^{-1} (Wang et al., 2015). Furthermore, AMA inhibition by ammonia might result in the accumulation of acetate up to inhibitory levels, thus contributing further to a negative feedback mechanism that eventually leads to complete reactor failure (Wang et al., 2015).

65 Under such high concentrations of ammonia and/or acetate, the so-called syntrophic
66 acetate oxidizing bacteria (SAOB) are able to reverse the homoacetogenic pathway and
67 convert acetate to carbon dioxide (CO_2) and hydrogen (H_2) (Schnürer et al., 1999). This
68 process is thermodynamically favourable through the concomitant consumption of H_2 by
69 HMA and, therefore, the syntrophic association between SAOB and HMA prevents the
70 inhibition of methanogenesis during the AD of nitrogen-rich substrates (Petersen and
71 Ahring, 1991). An increasing number of SAOB strains have been isolated in the recent
72 years and their physiology and genetics have been characterized quite thoroughly, but
73 information on the diversity, occurrence and role of SAOB in full-scale anaerobic digesters
74 is still limited (Westerholm et al., 2016). In an earlier integrative study based on the
75 metagenomic characterization of biomass and on the biogas isotopic profiling of different
76 industrial anaerobic digesters, we pointed out at the predominance of both HMA
77 communities and the hydrogenotrophic pathway in those digesters operated under
78 relatively high nitrogen loads (Ruiz-Sánchez et al., 2018). These conditions are conducive
79 to the enrichment of SAOB.

80 Here we aim at gaining a deeper insight into the microbial interactions, both of
81 metabolically active bacterial and archaeal populations that are potentially involved in the
82 SAO process. This new study focuses at the methanogenic biomass from an industrial
83 anaerobic digester treating nitrogen-rich agricultural wastes with no previous records of
84 process inhibition. A diversified research approach has been adopted for this purpose,
85 which combined batch methanogenic activity assays under different ammonia contents,
86 with Compound-Specific Isotope Analysis (CSIA) of $^{13}C/^{12}C$ natural isotopic fractionation of
87 CH_4 and CO_2 in the generated biogas, and the in-depth characterization of present and
88 metabolically active microbial populations by 16S-Illumina sequencing. The time-course

89 expression of relevant genes from bacteria (*16S* rRNA) and methanogenic archaea
90 (methyl coenzyme M reductase; *mcr*A) was quantified by qPCR.

91 MATERIALS AND METHODS

92 Batch experiments

93 Methanogenic biomass was collected from a 1,500 m^3 full-scale completely stirred tank
94 reactor (CSTR) for the anaerobic co-digestion of pig slurry and protein-rich agricultural
95 wastes (Vilasana, Lleida, Spain). This digester was operated according to the following
96 average parameters: total ammonia N (TAN) = 5.2 gN-TAN L^{-1}, chemical oxygen demand
97 (COD) = 101.2 gO_2 L^{-1}, volatile suspended solids (VSS) = 61.2 g L^{-1}, pH = 8.3, acetate
98 concentration = 0.0 gAc L^{-1}, hydraulic retention time (HRT) = 65 days, and temperature
99 within the mesophilic regime. Experiments were conducted in triplicate batch cultures (120
100 mL total volume, 60 mL working volume, inoculated with 12.7 gVSS L^{-1}), containing 1.0,
101 3.5 or 6.0 gN-TAN L^{-1} by adding NH_4Cl and 2.36 gAc L^{-1} as sodium acetate. Anaerobic
102 conditions were generated by flushing N_2 during 10 min. Cultures were incubated at 37^{0}C
103 under rotatory shaking and a bicarbonate buffer solution was added to maintain a constant
104 pH of 8 throughout the experiment. Control vials with neither acetate nor ammonia were
105 included to assess the endogenous CH_4 production of the inoculum.

106 Specific rates of acetate consumption and CH_4 production were determined and
107 expressed as gCOD $gVSS^{-1}$ d^{-1} (conversion factors: 2.857 mgCOD $mLCH_4^{-1}$; 1.067 gCOD
108 gAc^{-1}). For this purpose, samples of the liquid phase from each batch replicate (1 mL)
109 were collected after 0, 7, 11 and 17 days of incubation and directly centrifuged (4ºC,
110 20,000 rpm, 5 minutes). The supernatant (clarified fraction) was used for chemical
111 analysis, while the pellets (sedimented fraction) were kept at -80ºC until further processing
112 via molecular biology tools. Samples from the headspace of each culture were taken

periodically for the characterization of the biogas composition during the experiment. CH_4 yield ($mLCH_4\ gCOD^{-1}$), lag phase and specific CH_4 production rate (rCH_4; $mgCOD\ gVSS^{-1}\ d^{-1}$) were calculated after fitting the experimental data to the modified Gompertz equation. Samples of the accumulated biogas at the end of the incubation were collected for analysing the natural $^{13}C/^{12}C$ isotopic fractionation of CH_4 and CO_2. Gas/liquid volume changes due to sampling were taken into account in the calculation of mass balances.

Analytical methods

Total Kjeldhal Nitrogen (TKN), TAN and pH were determined according to the Standard Methods (APHA, 2005). The biogas was monitored along the experiment by sampling 100µl from headspace of each batch. Biogas composition (CH_4 and CO_2) and the concentration of individual volatile fatty acids (VFA) in the liquid media, including acetic (Ac), propionic, butyric, valeric and caproic acids, were measured in a gas chromatograph (Varian CP-3800). This instrument was equipped with a Varian Hayesep-Q 80-100 mesh capillary column and a TCD detector for the analysis of biogas, or a TRB-FFAP capillary column and a FID detector for the analysis of VFA.

CSIA of $^{13}C/^{12}C$ natural isotopic fractionation of biogas components was carried out by gas chromatography combustion–isotope ratio mass spectrometry (GC–IRMS). An Agilent 6890 gas chromatograph was fitted with a split/splitless injector and coupled to an isotope ratio mass spectrometer (Delta Plus Finnigan MAT) via a combustion interface (850°C), consisting of a 60 cm quartz tube (0.65 mm ID) filled with copper oxide. A liquid nitrogen cold trap was used to remove water. Separation was achieved on a CpsilCB (Chrompack) fused silica capillary column (60 m×0.32 mm; 0.12 µm film thickness) using He as carrier gas. The oven temperature was held at 40°C for 1 min, and increased to 320°C at a rate of 10°C min^{-1}. This final temperature was maintained for 25 minutes.

Squalene was used as internal standard. Each sample was run in triplicate to ensure reproducibility within ±0.2‰ (1σ), relative to the Vienna Pee Dee Belemnite (VPDB) standard. All carbon isotopic ratios were expressed as ‰ relative to the VPDB standard, and the apparent fractionation factor (αC) was determined according to Conrad et al., (2009). A αC within the range of 1.040 – 1.055 corresponded to a predominantly acetotrophic AD process, while that of 1.055 – 1.080 was mainly hydrogenotrophic (Conrad, 2005; Penning and Conrad, 2007).

Molecular methods

Total genomic DNA and RNA from all previously centrifuged biomass samples (pellets) were simultaneously extracted by an adapted protocol of the PowerMicrobiome™RNA Isolation kit (Qiagen). The RNA extracts were treated during 10 min at 25 °C with 10 units of DNase I to remove any contamination of genomic DNA, and directly subjected to a 16S rRNA-based PCR amplification to verify their purity (Prenafeta-Boldú et al., 2014). RNA extracts were subsequently transcribed to cDNA by means of PrimeScript™ RT reagent Kit (Perfect Real Time, Takara) following the manufacturer's instructions. cDNA and DNA extracts were kept frozen at −80 °C until further analysis.

Total and active bacterial populations and methanogenic archaea were quantified by means of qPCR amplification of *16S* rRNA and *mcrA* genes, respectively (Sotres et al., 2014). Reactions were carried out using the Brilliant II SYBR Green qPCR Master Mix (Stratagene) on a Real-Time PCR System Mx3000P (Stratagene). The specificity of the qPCR amplifications was determined by observations of the corresponding melting curves and gel electrophoresis profiles. To prepare the corresponding standard curves two duplex DNA were synthesized (Metabion GmbH). Ten-fold serial dilutions of both standard genes

were subjected to qPCR assays in duplicate showing a linear response between 10^1 and 10^8 gene copy numbers. The qPCR standards for both genes fitted quality standards with amplification efficiencies between 90 and 110% and R^2 above 0.985. All results were processed by the MxPro™ QPCR software (Stratagene). All results obtained from triplicate independent batches were treated statistically. The Shapiro-Wilk test was performed to determine whether data were normally distributed. Considering the paired structure and normal distribution of the data, an analysis of variance (ANOVA) was performed. The combination of factors were the sampling time (0, 7, 11 and 17 days) and the TAN treatments (1.0, 3.5 and 6.0 gN-TAN). Subsequently, pairwise comparisons Fisher's least significant difference (LSD) were applied to test differences between batches by sampling periods. The significance threshold was established at 0.05 type I error. All statistical analysis were performed by means of XLSTAT 2018 software (Addinsoft) and SigmaPlot 11.0 software.

The time course evolution of methanogenic activity and expression of 16S rRNA and *mcrA* genes determined the sampling periods for high throughput sequencing. The microbial community structure was characterized by 16S-Illumina sequencing analysis after 11 and 17 days, respectively for batches exposed to 1.0, 3.5, and 6.0 gN-TAN L^{-1}, when the maximum CH_4 production rates and gene expression level was recorded (Figures 1 and 2). Microbial diversity in the bacteria and archaea domains was assessed in duplicate by means of *16S* rRNA Illumina (MiSeq) high-throughput sequencing as described previously (Pelissari et al., 2017). The obtained DNA and cDNA reads were compiled in FASTq files for further bioinformatic processing. Trimming of the 16S rRNA barcoded sequences into libraries was carried out using the QIIME software version 1.8.0 and quality filtering of the reads was performed at Q25, prior to their grouping into Operational Taxonomic Units (OTUs) at a 97% sequence homology cut-off. OTUs were then taxonomically classified

using the RDP Naïve Bayesian Classifier (2.2) with a bootstrap cut-off value of 80%, and compiled to each taxonomic level.

The number of observed OTUs, Goods coverage, alpha biodiversity parameters (the inverted Simpson and Shannon indexes), and species richness (Chao1 estimator) were calculated using the Mothur software v.1.35.9 (http://www.mothur.org). The number of reads were rarefacted to the lowest number among the different samples. The sequence data from the MiSeq NGS assessment were submitted to the Sequence Read Archive (SRA) of the National Center for Biotechnology Information (NCBI) under the study accession number PRJNA385091.

RESULTS AND DISCUSSION

Batch incubation experiments

Methanogenic activity assays

The time-course evolution of acetate and CH_4 was monitored at low, intermediate and high ammonia exposure (1.0, 3.5, and 6.0 gN-TAN L^{-1}) in batches that were inoculated with freshly collected biomass from the studied agricultural anaerobic digester (Figure 1). The estimated FAN concentrations at the tested intermediate and high ammonia exposure were above the inhibitory threshold for methanogenesis (Table 1), considering that values as low as 250 mg L^{-1} have been found to impair the anaerobic digestion process with unaclimated biomass (Yenigün and Demirel, 2013). The specific acetate uptake rate (*r*Ac) was similar up to 3.5 gN-TAN L^{-1} but it decreased by 46% at 6.0 gN-TAN L^{-1} (Table 1). The impact of ammonia on methanogenesis was also significant since the CH_4 production rate (rCH_4) decreased by 26% and 31% upon ammonia exposure at 3.5 and 6.0 gN-TAN L^{-1}, with respect to the rCH_4 at 1 gN-TAN L^{-1} (Table 1). This apparent ~~higher~~ vulnerability of acetate-utilizing microorganisms might be the result of the well-known susceptibility of

AMA to ammonia (Hunik et al., 1990). Under such conditions, acetate might also be consumed by the SAOB but this metabolic process has been associated to relatively low conversion rates (Sun et al., 2014). Along with a high ammonia content, those digesters were often characterized by a prolonged biomass retention time and thermophilic temperature, parameters that have been identified as crucial for the enrichment of the rather slow-growing SAO microbial communities (Sun et al., 2014). However, despite the lower metabolic rates under high ammonia concentrations, all tested batches reached a similar CH_4 yield and more than the 80% of the added acetate was eventually recovered as CH_4 in terms of COD equivalents.

Isotopic fractionation of biogas

Most of the previous studies on the application of isotopic analysis of biogas for the characterization of anaerobic digesters subjected to high ammonia levels were based on using radioactive (Karakashev et al., 2006; Sun et al., 2014) or stable (Mulat et al., 2014) isotope-labelling at the acetate methyl group. The protocol implemented in this study based on CSIA of $^{13}C/^{12}C$ natural isotopic fractionation provided a deeper insight on the methanogenic pathways, without the need of using expensive and/or dangerous labelled substrates. The apparent fractionation factor α_C as defined by Whiticar and Faber (1986) from the measured δCH_4 and δCO_2, and later reviewed by (Conrad et al., 2009) was used. This factor indicates that environments with a $\alpha_C<1.055$ are dominated by AMA, while those with a $\alpha_C>1.065$ point to the predominance of HMA (up to exclusive hydrogenotrophy at $\alpha_C=1.085$). From the α_C values calculated in the present study, it can be concluded that increasing the ammonia content prompted a metabolic shift in methanogenesis from AMA at 1.0 gN-TAN L^{-1} to a HMA activity that was predominant at 3.5 gN-TAN L^{-1}, and even exclusive at 6.0 gN-TAN L^{-1} (Table 1). This shift from acetotrophic to hydrogenotrophic methanogenesis is consistent with previous observations

from anaerobic digesters under increasing ammonia concentrations (Wang et al., 2015). Concurrent prevalence of hydrogenotrophy along with consumption of acetate (added as the sole electron source), strongly supports the hypothesis that biomass from the studied anaerobic digester contained SAO species that were active under a relatively high ammonia content. Furthermore, these results also indicate that, despite its previous history of acclimation and adaptation to high nitrogen loads, the methanogenic biomass was still able to modulate the metabolism towards acetotrophy when exposed to low concentrations of ammonia.

Microbial community analysis

Quantitative expression profile of selected functional genes

The effect of ammonia on the expression ratio (qPCR quantification of transcripts versus gene copies) of specific functional genes from bacteria (*16S* rRNA) and methanogenic archaea (*mcr*A) was consistent with the previously observed profiles of acetate consumption and CH_4 generation (Figure 1). The bacterial *16S* rRNA expression ratio increased in time, reaching a maximum value at around day 11 that was maintained until the end of incubations at day 17 (Figure 2a). This maximum expression ratio was a 53% lower at 6.0 gN-TAN L^{-1}, in relation to that of 1.0 gN-TAN L^{-1} (differences between 1.0 and 3.5 gN-TAN L^{-1} were not significant). Despite the fact that the expression of ribosomal genes must be regarded as a global metabolic indicator for all bacteria, and so it cannot univocally be associated to the acetotrophic activity, it might partly explain the reduction in *r*Ac that occurred at high ammonia concentrations (Table 1).

For the archaea, instead, a much more specific gene directly related to methanogenesis was targeted. The expression ratio of *mcr*A genes at low and intermediate ammonia concentrations (1.0 – 3.5 gN-TAN L^{-1}) was very similar (Figure 2b). The observed values

were rather low during the first 5 days of incubation but they sharply peaked at around day 11, to decrease again at day 17. Such unimodal profile fits the observed lag-phase in CH_4 production of approximately 6 days and the exponential phase in CH_4 accumulation that followed, before the declining phase that started shortly after day 11. Incubations with the highest ammonia concentration (6.0 gN-TAN L^{-1}) resulted in a *mcr*A expression ratio that was a 83% lower than those at low and intermediate ammonia exposure (Figure 2b). As discussed previously, these batches showed the longest lag-phases and the lowest *r*CH_4 production, but similar CH_4 yields were eventually achieved.

Bacterial community structure and response to ammonia exposure

The microbial community structure from the most active period during the batch activity assays was assessed by high throughput DNA sequencing. A total of 440,756 and 224,133 high quality *16S* rRNA ribosomal genes and transcripts (cDNA) reads were obtained for the *Bacteria* domain. These reads were grouped into operational taxonomic units (OTUs, defined at 97% sequence homology cut-off) and confidently assigned to specific taxa (Table 2). The Good's coverage estimator on the percentage of the total species (as OTUs) represented at any given sample was above 99%, indicating that the observed bacterial species encompassed most of the samples' populations. Species biodiversity (Shannon and inverted Simpson indexes) and richness (Chao1) were rather similar among samples, with an estimated number of species in the inoculum of 5,592. Species richness in active bacterial populations (cDNA ribotype libraries) was always lower than that corresponding to the present species (DNA ribotype libraries), but the biodiversity of the active population increased upon ammonia exposure. This indicates that an important proportion of the species from the inoculum were metabolically active under the tested conditions, and that ammonia triggered the response of an increasingly complex bacterial community.

284 The bacterial community structure, based on 16S rRNA gene counts, remained relatively
285 stable during all assays regardless of the TAN concentration (Figure 3a). Representatives
286 of the order *Anaerolineales* were predominant, with a relative gene abundance (RGA) of
287 more than 40% in all assays. Other important groups included members of the orders
288 *Clostridiales* (16% RGA) and *Bacteroidales* (9–12% RGA), the former being particularly
289 relevant as it encompasses most of the recently described SAOB. In our previous
290 metagenomic study (Ruiz-Sánchez et al., 2018) we suggested that members of phyla
291 *Bacteroidetes*, along with *Chloroflexi*, might encompass yet undescribed SAOB.

292 In contrast with this stable microbial community structure, a population shift was observed
293 in the active species when exposed to increasing ammonia concentrations. In terms of
294 relative transcript abundance (RTA), members of the *Clostridiales* (22–26% RTA) and
295 *Anaerolineales* (14–20% RTA) were among the most active communities. Other relevant
296 metabolically active groups were found in the *Bacteroidales* (9–12% RTA), *Burkholderiales*
297 (5–8% RTA), *Pseudomonadales* (5–7% RTA) and *Planctomycetales* (3% RTA). In contrast
298 to these groups, which displayed little sensitivity to ammonia, *Sphingobacteriales* showed
299 a clear negative correlation with the concentration of ammonia, so that their RTA
300 decreased from 15% to 1% upon an ammonia supplementation from 1.0 to 6.0 gN-TAN L^{-1}
301 .

302 The high throughput sequencing data from this study was also mined for the presence of
303 well-known SAOB (Fotidis et al., 2013). OTUs homologous to the
304 thermotolerant/thermophilic *Tepidanaerobacter acetatoxydans* and *Thermacetogenium*
305 *phaeum* were detected, but in very low abundance and only in certain samples. Therefore,
306 these particular thermophilic species played a minor role in the studied mesophilic reactor.
307 Nevertheless, the proven hydrogenotrophy at relatively high TAN levels and the absence

of acetate accumulation, suggested that other non-described mesophilic SAO microbial communities must be active in the biomass.

The *16S* rRNA gene expression ratio (transcripts to genes) at intermediate and high ammonia levels (3.5 and 6.0 gN-TAN L^{-1}), in relation to that of the basal concentration (1.0 gN-TAN L^{-1}) gives a further insight on the response of relevant bacterial species (as OTUs) to ammonia exposure (Figure 4). The highest expression shift along with increasing TAN concentrations was observed for a number of OTUs related to the genera *Thioalkalispira*, *Caulobacter*, *Bellilinea*, *Clostridium*, *Leptolinea*, *Bacteroides* and *Acetivibrio*; while representatives of the genera *Natronoanaerobium*, *Sphingobacterium*, and *Synergistes* appeared to be inhibited at 6.0 gN-TAN L^{-1}. Individual BLAST searches from the sequences of the "ammonia-philic" OTUs yielded uncultured bacteria from a variety of anaerobic digesters that might have been exposed to relatively high ammonia levels (Table 3). Of particular interest is OTU1, which appears to be somewhat related to the genus *Longilinea* (94% sequence homology) and was by far the most abundant ammonia-responding OTU (30% in RTA). The second most active species (OTU2, 8% in RTA), also belonged to the class *Anaerolineae* (*Chloroflexi*), and displayed its highest similarity to a member of the genus *Leptolinea* (88% sequence homology). Four additional OTUs affiliated within the same class (genera *Levilinea* and *Bellilinea*) also increased their relative activity in the presence of ammonia, but their abundance was significantly lower. The class *Anaerolineae* was described in order to accommodate four new isolates originating from mesophilic UASB reactors (*Levilinea saccharolytica* and *Leptolinea tardivitalis*) (Yamada et al., 2006), a rice paddy soil (*Longilinea arvoryzae*), and a thermophilic digester (*Bellilinea caldifistulae*) (Yamada et al., 2007). They have relatively prolonged doubling times (45 – 92 h) and differ in their optimal temperature for growth, which could explain the low occurrence of the thermophilic *Bellilinea* in the mesophilic

reactor. Interestingly, *Longilinea* and *Bellilinea* share the fact that growth is enhanced in co-cultivation with hydrogenotrophic methanogens. Nevertheless, neither H_2/CO_2 nor acetate served as sole carbon sources for growth in pure cultures, so that their potential role as SAOB might be put into question.

A ribotype distantly related to *Bacteroides* (OTU3) could also have played a relevant role in the anaerobic digestion of nitrogen-rich substrates, given its relatively high expression level (8% RA of ribosomal transcripts). Despite poor phylogenetic definition, OTU3 exhibits a relatively high sequence similarity to several uncultured bacteria from anaerobic digesters, including an anaerobic sequencing batch reactor (SBR) treating swine waste at 4.9 g N-TAN L^{-1} (Angenent et al., 2002). A number of unidentified clostridia (OTUs 7, 16, and 31) with a significant presence in the methanogenic biomass (>1%) increased their relative expression under high ammonia concentrations, and revealed high sequence similarity with ribotypes previously reported in other ammonia-rich anaerobic digesters. It could thus well be that some of the above mentioned OTUs correspond to yet undescribed SAOB.

Archaeal community structure and response to ammonia exposure

High throughput DNA sequencing of the *Archaea* yielded 401,486 genes and 444,516 transcript reads. As with the bacteria, the Good's coverage estimator for the archaea was above 99%, but the Chao1 estimator was one order of magnitude lower, with a predicted 414 archaeal species in the original inoculum. Both the biodiversity and number of active archaea were always lower than those corresponding to the present species (DNA ribotype libraries) so that, contrary on the bacteria, an increasing ammonia exposure generated a less diversified response of the archaeal community. The original methanogenic biomass (inoculum) was primarily composed by strict hydrogenotrophic

orders, such as *Methanomicrobiales* (*Methanoculleus*, 31% RGA) and *Methanobacteriales* (*Methanobrevibacter*, 26% RGA), but also the metabolically versatile *Methanosarcinales* (30% RGA), which encompasses both facultative and obligate acetotrophic genera (*Methanosarcina* and *Methanosaeta*). Representatives of the thermophilic chemolithoautotrophic ammonia oxidizing archaeon *Nitrosocaldus* were also present at a lower yet relevant abundance (7% RGA). Contrary to the bacteria, a significant population shift was observed for the archaea after incubations, in terms of gene counts (RGA), along with increasing ammonia concentrations. *Methanosaeta* decreased from 10% RGA at 1.0 gN-TAN L^{-1} to less than 3% at 6.0 gN-TAN L^{-1}, while representatives of *Methanomassiliicoccus* (order *Methanomassiliicoccales*) where enriched from 11% RGA (1.0 gN-TAN L^{-1}) up to 31% RGA (6.0 gN-TAN L^{-1}). This novel order of methyl-dependent hydrogenotrophic methanogens encompasses the former, recently reclassified, *Thermoplasmatales* (Adam et al., 2017; Borrel et al., 2014). Species from the *Methanomassiliicoccales* have recently been found in various anaerobic environments and are becoming an emerging research subject due to their scarcely known biology (Ziganshin et al., 2016).

The profiles of active archaea were rather similar at 1.0 and 3.5 gN-TAN L^{-1}, with *Methanosaeta* (48%–40% RTA) and *Methanoculleus*, (40%–47% RTA) as the most active genera (Figure 3b). *Methanoculleus* maintained a rather high level of gene expression regardless of ammonia exposure (about 45% RTA), but activity increased significantly for *Methanomassiliicoccus* (36% RTA) at 6.0 gN-TAN L^{-1}. This finding further confirms that hydrogenotrophy had become the predominant methanogenic process at a high ammonia content, as seen previously from the isotopic fractionation profiles (Table 1). Furthermore, the extraordinary growth and activity levels of *Methanomassiliicoccus* indicates that this

particular taxon plays a vital role in the anaerobic digestion process under the tested high ammonia conditions and, therefore, it deserves further attention.

Recent genomic evidence points out to a number of physiological and metabolic features of the *Methanomassiliicoccales* that are relevant for this study. To start with, this order is characterized by the presence of quaternary ammonium efflux pumps (Borrel et al., 2014), which might explain why it thrived under high ammonia concentrations. They also lack the methyl-branch of the archaeal type Wood–Ljungdahl pathway and the coenzyme M methyltransferase complex (MTR), which makes them reliant on methyl-dependent hydrogenotrophic methanogenesis (Adam et al., 2017). Interestingly, the *Methanomassiliicoccales* have the genetic capability of heterotrophic growth on acetate and, possibly, of synthesizing acetyl-CoA from formate and CO_2 (Lang et al., 2015). These findings are in agreement with metagenomic evidence that species in the *Methanomassiliccoccales* harbour several genes related to acetyl-CoA pathway (Campanaro et al., 2016). Species in this taxon might therefore be able to transform acetate to CO_2, but they also possesses the *fhd*A gene encoding a glutathione-dependent formaldehyde dehydrogenase that transform formaldehyde to formate. Additionally, a recent study on the evolution of the bifunctional enzyme acetyl-CoA synthase/carbon monoxide dehydrogenase gene cluster (ACS/CODH) claimed that the *Methanomassiliicoccales* have a bacterial-type CODH, likely due to ancient interdomain transfer events (Adam et al., 2018). The CODH enzymes are used by aerobic and anaerobic carboxytrophs to catalyze the reversible conversion between CO_2 and CO. Remarkably, in the *Methanomassiliicoccales*, these enzymes only function in the oxidative direction due to their inability of carbon fixation.

Hence, considering the relevance of the predominant OTUs affiliated to *Methanomassiliccocales* from the present study, an *in silico 16S* rRNA assessment with

406 different databases (RDP, GreenGenes and BLAST) was performed. As a result, the
407 affiliation of OTU4 to the *Methanomassiliicoccales*, and more specifically to the genus
408 *Methanomassiliicoccus*, was confirmed. We propose a novel archaeal syntrophic
409 association between species in the genus *Methanoculleus*, which have consistently been
410 reported to prevail in ammonia-enriched anaerobic digesters dominated by the SAO
411 process (Sun et al., 2014), and *Methanomassiliicoccus*. The latter would then acts as
412 archaeal SAO, analogue to the known SAOB, by converting acetate to formate and/or
413 CO_2, substrates that would then be consumed by *Methanoculleus*. The association
414 between *Methanomassiliicoccus* and *Methanoculleus* has already been reported in an
415 anaerobic digestor treating food waste, where their dominance was strongly correlated
416 with accumulation of VFA, increasing OLR, and concentration of ammonia (Li et al., 2018).

417 **CONCLUSIONS**

418 Biomass from a full-scale anaerobic digester adapted to relatively high ammonia
419 concentrations was able to swiftly change its metabolic mode from acetotrophic to
420 hydrogenotrophic methanogenesis upon increasing ammonia levels, by
421 activating/deactivating specific microbial populations. Biological activity was negatively
422 affected at the highest tested ammonia concentration (6.0 gN-TAN L^{-1}), both in terms of
423 CH_4 production and acetate consumption rates, as well as in relation to a decreasing
424 expression level of bacteria and methanogenic archaea, but a similar CH_4 yield was
425 eventually achieved with all tested nitrogen conditions.

426 In contrast to the bacterial community structure, which remained relatively stable during
427 the experiments, important changes for the active species were observed in response to
428 ammonia. Despite the strong evidence for the occurrence of the SAO process under high
429 ammonia concentrations, none of the SAOB that are currently known from the literature

played a significant role in the studied biomass. However, several bacteria belonging to taxa that have previously been associated to acetate metabolism were stimulated upon ammonia exposure. Concerning the methanogenic archaea, the strictly acetotrophic genus *Methanosaeta* was among the most active under low ammonia concentrations (1.0 gN-TAN L^{-1}). However, *Methanosaeta* quickly declined both in biomass abundance and in activity at higher ammonia levels, and was overtaken by representatives of the hydrogenotrophic genera *Methanoculleus* and *Methanomassiliicoccus*. Such archaeal association could be explained by the extraordinary metabolic flexibility and complementary of these two genera, which contribute to both acetotrophy and hydrogenotrophy.

Acknowledgements

This work was supported by Spanish government under the INIA project *"PROGRAMO Advanced anaerobic treatment of wastes with high lipid/protein content, with ammonia recovery"* program no. (RTA2012-00098-00-00). The first author has a grant from Spanish government (FPI-INIA RTA2012-00098-00-00). IRTA thanks the financial support of CERCA program of the Generalitat de Catalunya.

REFERENCES

American Public Health Association (APHA) (2005) Standard method for examination of water and wastewater, 21st edn. APHA, AWWA, WPCF, Washington

Adam PS, Borrel G, Brochier-Armanet C, Gribaldo S. 2017. The growing tree of Archaea: New perspectives on their diversity, evolution and ecology. *ISME J.*

Adam PS, Borrel G, Gribaldo S. 2018. Evolutionary history of carbon monoxide dehydrogenase/acetyl-CoA synthase, one of the oldest enzymatic complexes. *Proc.*

454 *Natl. Acad. Sci.*:201716667.
455 Angenent LT, Sung S, Raskin L. 2002. Methanogenic population dynamics during startup
456 of a full-scale anaerobic sequencing batch reactor treating swine waste. *Water Res.*
457 **36**:4648–4654.
458 Banks CJ, Zhang Y, Jiang Y, Heaven S. 2012. Trace element requirements for stable food
459 waste digestion at elevated ammonia concentrations. *Bioresour. Technol.* **104**:127–
460 135.
461 Borrel G, Parisot N, Harris HMB, Peyretaillade E, Gaci N, Tottey W, Bardot O, Raymann
462 K, Gribaldo S, Peyret P, O'Toole PW, Bruge`re JF. 2014. Comparative genomics
463 highlights the unique biology of Methanomassiliicoccales, a Thermoplasmatales-
464 related seventh order of methanogenic archaea that encodes pyrrolysine. *BMC*
465 *Genomics* **15**.
466 Campanaro S, Treu L, Kougias PG, De Francisci D, Valle G, Angelidaki I. 2016.
467 Metagenomic analysis and functional characterization of the biogas microbiome using
468 high throughput shotgun sequencing and a novel binning strategy. *Biotechnol.*
469 *Biofuels* **9**:26.
470 Conrad R. 2005. Quantification of methanogenic pathways using stable carbon isotopic
471 signatures: A review and a proposal. *Org. Geochem.* **36**:739–752.
472 Conrad R, Claus P, Casper P. 2009. Characterization of stable isotope fractionation during
473 methane production in the sediment of a eutrophic lake, Lake Dagow, Germany.
474 *Limnol. Oceanogr.* **54**:457–471.
475 Demirel B, Scherer P. 2008. The roles of acetotrophic and hydrogenotrophic methanogens
476 during anaerobic conversion of biomass to methane: A review. *Rev. Environ. Sci.*
477 *Biotechnol.* **7**:173–190.
478 Fotidis IA, Karakashev D, Angelidaki I. 2013. Bioaugmentation with an acetate-oxidising

consortium as a tool to tackle ammonia inhibition of anaerobic digestion. *Bioresour. Technol.* **146**:57–62.

Hunik JH, Hamelers HVM, Koster IW. 1990. Growth-rate inhibition of acetoclastic methanogens by ammonia and pH in poultry manure digestion. *Biol. Wastes* **32**:285–297.

Karakashev D, Batstone DJ, Trably E, Angelidaki I. 2006. Acetate oxidation is the dominant methanogenic pathway from acetate in the absence of Methanosaetaceae. *Appl. Environ. Microbiol.* **72**:5138–5141.

Lang K, Schuldes J, Klingl A, Poehlein A, Daniel R, Brune A. 2015. New mode of energy metabolism in the seventh order of methanogens as revealed by comparative genome analysis of "Candidatus Methanoplasma termitum." *Appl. Environ. Microbiol.* **81**:1338–1352.

Lettinga G. 2010. Challenges of a feasible route towards sustainability in environmental protection. *Front. Environ. Sci. Eng. China* **4**:123–134.

Li Q, Yuwen C, Cheng X, Yang X, Chen R, Wang XC. 2018. Responses of microbial capacity and community on the performance of mesophilic co-digestion of food waste and waste activated sludge in a high-frequency feeding CSTR. *Bioresour. Technol.* **260**:85–94. http://www.sciencedirect.com/science/article/pii/S0960852418304498.

Li, Y., Leahy, S. C., Jeyanathan, J., Henderson, G., Cox, F., Altermann, E., … Attwood, G. T. (2016). The complete genome sequence of the methanogenic archaeon ISO4-H5 provides insights into the methylotrophic lifestyle of a ruminal representative of the Methanomassiliicoccales. *Standards in Genomic Sciences*, **11:**59.

Mulat DG, Ward AJ, Adamsen APS, Voigt NV, Nielsen JL, Feilberg A. 2014. Quantifying contribution of synthrophic acetate oxidation to methane production in thermophilic anaerobic reactors by membrane inlet mass spectrometry. *Environ. Sci. Technol.*

504 **48**:2505–2511.
505 Nordgård A, 2017. Microbial community analysis in developing biogas reactor technology
506 for Norwegian agriculture (Doctoral thesis). Retrieved from
507 https://brage.bibsys.no/xmlui/
508 Pelissari C, Guivernau M, Viñas M, de Souza SS, García J, Sezerino PH, Ávila C. 2017.
509 Unraveling the active microbial populations involved in nitrogen utilization in a vertical
510 subsurface flow constructed wetland treating urban wastewater. *Sci. Total Environ.*
511 **584**–**585**:642–650.
512 Penning H, Conrad R. 2007. Quantification of carbon flow from stable isotope fractionation
513 in rice field soils with different organic matter content. *Org. Geochem.* **38**:2058–2069.
514 Petersen SP, Ahring BK. 1991. Acetate Oxidation in A Thermophilic Anaerobic Sewage-
515 Sludge Digester - the Importance of Non-Aceticlastic Methanogenesis from Acetate.
516 *Fems Microbiol. Ecol.* **86**:149–157.
517 Prenafeta-Boldú FX, Rojo N, Gallastegui G, Guivernau M, Viñas M, Elías A. 2014. Role of
518 Thiobacillus thioparus in the biodegradation of carbon disulfide in a biofilter packed
519 with a recycled organic pelletized material. *Biodegradation* **25**:557–568.
520 Ruiz-Sánchez J, Campanaro S, Guivernau M, Fernández B, Prenafeta-Boldú FX. 2018.
521 Effect of ammonia on the active microbiome and metagenome from stable full-scale
522 digesters. *Bioresour. Technol.* **250**:513–522.
523 Schnürer A, Nordberg Å. 2008. Ammonia, a selective agent for methane production by
524 syntrophic acetate oxidation at mesophilic temperature. *Water Sci. Technol.* **57**:735–
525 740.
526 Schnürer A, Zellner G, Svensson BH. 1999. Mesophilic syntrophic acetate oxidation during
527 methane formation in biogas reactors. *FEMS Microbiol. Ecol.* **29**:249–261.
528 Sotres A, Díaz-Marcos J, Guivernau M, Illa J, Magrí A, Prenafeta-Boldú FX, Bonmatí A,

529 Viñas M. 2014. Microbial community dynamics in two-chambered microbial fuel cells:
530 Effect of different ion exchange membranes. *J. Chem. Technol. Biotechnol.*:n/a-n/a.
531 Sun L, Müller B, Westerholm M, Schnürer A. 2014. Syntrophic acetate oxidation in
532 industrial CSTR biogas digesters. *J. Biotechnol.* **171**:39–44.
533 Wang H, Fotidis IA, Angelidaki I. 2015. Ammonia effect on hydrogenotrophic methanogens
534 and syntrophic acetate-oxidizing bacteria. *FEMS Microbiol. Ecol.* **91**.
535 Westerholm M, Moestedt J, Schnürer A. 2016. Biogas production through syntrophic
536 acetate oxidation and deliberate operating strategies for improved digester
537 performance. *Appl. Energy*.
538 Whiticar MJ, Faber E. 1986. Methane oxidation in sediment and water column
539 environments-Isotope evidence. *Org. Geochem.* **10**:759–768.
540 Yamada T, Imachi H, Ohashi A, Harada H, Hanada S, Kamagata Y, Sekiguchi Y. 2007.
541 Bellilinea caldifistulae gen. nov., sp. nov and Longilinea arvoryzae gen. nov., sp. nov.,
542 strictly anaerobic, filamentous bacteria of the phylum Chloroflexi isolated from
543 methanogenic propionate-degrading consortia. *Int. J. Syst. Evol. Microbiol.* **57**:2299–
544 2306.
545 Yamada T, Sekiguchi Y, Hanada S, Imachi H, Ohashi A, Harada H, Kamagata Y. 2006.
546 Anaerolinea thermolimosa sp. nov., Levilinea saccharolytica gen. nov., sp. nov. and
547 Leptolinea tardivitalis gen. nov., sp. nov., novel filamentous anaerobes, and
548 description of the new classes Anaerolineae classis nov. and Caldilineae classis nov.
549 in the . *Int. J. Syst. Evol. Microbiol.* **56**:1331–1340.
550 Yenigün O, Demirel B. 2013. Ammonia inhibition in anaerobic digestion: A review. *Process*
551 *Biochem.* **48**:901–911.
552 Ziganshin AM, Ziganshina EE, Kleinsteuber S, Nikolausz M. 2016. Comparative analysis
553 of methanogenic communities in different laboratory-scale anaerobic digesters.

Archaea **2016**.

TABLE LEGENDS

Table 1. Results of the batch activity assays at different ammonia concentration in relation to the Specific rates of acetate consumption (*r*Ac) and methane production (*r*CH4), lag phase, methane yield and the apparent fractionation factor (αC). Depicted values correspond to the average and standard deviation of three independent replicates.

Table 2. Estimators of microbial species diversity/richness based on NGS of 16S rRNA genes and transcripts from the *Bacteria* and *Archaea* domains, obtained from the initial inoculum and after incubation during 11 and 17 days under increasing TAN concentrations. Predominant assigned genera (relative abundance > 5%) are also listed.

Table 3. Best match in BLAST searches (GenBank, NCBI, USA) on TAN-responding bacterial OTUs (see Figure 4). Only OTUs with a relative abundance in the original methanogenic biomass higher than 1% are listed.

LEGENDS TO FIGURES

Figure 1. Evolution of acetic acid (asterisks) and CH_4 (squares), both expressed as mg of COD equivalents, in batch reactors incubated at different TAN concentrations: (A) 1.0 gN-TAN L^{-1}; (B) 3.5 gN-TAN L^{-1}; and (C) 6.0 gN-TAN L^{-1}. The Gompertz equation (dashed line) was fitted to experimental methane yields (circles). Measured data are expressed as the average (sign) and the standard deviation (bars) of three independent batches.

Figure 2. Time-course quantitative PCR results from biomass samples of three independent batches incubated at 1.0, 3.5, and 6.0 gN-TAN L^{-1} (squares, circles, and triangles). The average (signs) and standard deviation (bars) of the ratio between number of transcripts and gene copies for the bacterial 16S rRNA (A) and the archaeal *mcrA* (B) has been depicted. Statistical significance in pairwise comparisons (n=3, p<0.05) in relation to the lowest ammonia exposure have been highlighted with an asterisk.

Figure 3. Relative abundance of bacterial (A) and archaeal (B) 16S rRNA genes and transcripts, expressed respectively at the order and genus phylogenetic level, in methanogenic batch reactors supplemented with increasing ammonia concentrations (1.0, 3.5, and 6.0 gN-TAN L^{-1}), and after different incubation times (0, 11, and 17 days). Each bar represents the average of two independent batches.

Figure 4. Ratio between the relative expression level of bacterial 16S rRNA transcripts obtained in batch methanogenic assays incubated at 3.5 gN-TAN L^{-1} (grey bar) and 6 gN-TAN L^{-1} (black bar), in relation to that at 1 gN-TAN L^{-1}. Assigned taxon and OTU number (in brackets) are indicated. Only the species with a relative abundance higher than 0.3% have been depicted.

Table 1

TAN ($gN\ L^{-1}$)	FAN [a] ($mgN\ L^{-1}$)	rAc [b] ($mgCOD\ gVSS^{-1}\ d^{-1}$)	rCH$_4$ [c] ($mgCOD\ gVSS^{-1}\ d^{-1}$)	Lag phase [c] (d)	Methane yield [c] ($mLCH_4\ gCOD^{-1}$)	αC [d]	Predominant methanogenic pathway [d]
1.0	114	16.80±0.42	13.61±0.25	6.37±0.15	238.41± 9.76	1.054±0.017	Acetotrophic
3.5	399	16.93±0.35	12.71±0.26*	6.28±0.13	245.63±13.54	1.077±0.001*	Hydrogenotrophic
6.0	683	9.10±0.35*	9.86±0.02*	10.17±0.10*	251.15± 2.21	1.080±0.000*	Exclusively hydrogenotrophic

[a] Calculated from the ammonium/ammonia chemical equilibrium in water at pH = 8 and T = 37°C.
[b] Measured empirically.
[c] From the mathematical fitting to the Gompertz equation (n=21, r^2>0.98).
[d] According to Conrad (2005).
* Statistically significant differences in relation to 1.0 gN-TAN L^{-1} (n=3, p<0.05).

Table 2

.

Parameter	Microbial group	Inoculum	1.0 g N-TAN L^{-1}		3.5 g N-TAN L^{-1}		6.0 g N-TAN L^{-1}	
			Genes	Transcripts	Genes	Transcripts	Genes	Transcripts
No. of reads	Bacteria	217,432	85,745	53,318	68,355	112,479	69,224	58,836
	Archaea	193,179	54,798	134,018	68,513	141,590	84,996	168,908
No. of OTUs [a]	Bacteria	4,720	3,241	2,032	3,110	3,514	3,105	2538
	Archaea	373	282	183	325	185	211	201
Coverage [b] (%)	Bacteria	99.42	99.90	99.87	99.85	99.92	99.88	99.85
	Archaea	99.97	99.89	99.96	99.92	99.96	99.92	99.97
Shannon (diversity)	Bacteria	4.05	3.89	4.30	4.02	4.64	3.92	4.62
	Archaea	2.72	2.39	1.48	2.37	1.52	2.13	1.70
Simpson (diversity)	Bacteria	8.76	7.66	24.03	8.21	24.37	7.31	26.68
	Archaea	8.02	6.73	2.80	5.71	3.11	4.93	3.34
Chao1 (richness) [c]	Bacteria	5,592 (64)	5,047 (127)	3,364 (116)	4,927 (126)	4,516 (77)	4,974 (130)	3,760 (99)
	Archaea	414 (14)	362 (25)	258 (28)	383 (17)	272 (33)	338 (44)	243 (16)
Predominant genera (% relative abundance)	Bacteria	*Longilinea* (36) *Clostridium* (10) *Bacteroides* (9) *Leptolinea* (7)	*Longilinea* (39) *Leptolinea* (11) *Clostridium* (9) *Bacteroides* (6)	*Alkaliphilus* (13) *Sphingobacterium* (11) *Leptolinea* (9) *Levilinea* (6) *Mariniphaga* (6) *Synergistes* (6) *Pseudomonas* (6)	*Longilinea* (38) *Clostridium* (9) *Bacteroides* (8) *Leptolinea* (6)	*Alkaliphilus* (17) *Sphingobacterium* (11) *Leptolinea* (6) *Pseudomonas* (6) *Mariniphaga* (5)	*Longilinea* (40) *Bacteroides* (10) *Clostridium* (9) *Synergistes* (5)	*Alkaliphilus* (17) *Leptolinea* (8) *Pseudomonas* (7) *Symbiobacterium* (6) *Levilineaca* (5) *Mariniphaga* (5)
	Archaea	*Methanoculleus* (31) *Methanobrevibacter* (26) *Methanosarcina* (20) *Methanosaeta* (10) *Nitrosocaldus* (7)	*Methanoculleus* (39) *Methanosarcina* (16) *Methanosaeta* (15) *Methanobrevibacter* (12) *Methanomassiliicoccus* (11)	*Methanosaeta* (48) *Methanoculleus* (40) *Methanomassiliicoccus* (7)	*Methanoculleus* (39) *Methanomassiliicoccus* (22) *Methanosarcina* (16) *Methanosaeta* (9) *Methanobrevibacter* (7)	*Methanosaeta* (40) *Methanoculleus* (47) *Methanomassiliicoccus* (9)	*Methanoculleus* (35) *Methanomassiliicoccus* (31) *Methanosarcina* (14) *Methanobrevibacter* (8)	*Methanoculleus* (45) *Methanomassiliicoccus* (36) *Methanosaeta* (10)

[a] Observed number of species based on operational taxonomic units (at 97% sequence homology cut-off).
[b] Good's estimator of coverage calculated as (1−(singletons/reads)) × 100.
[c] Estimated number of species average and standard deviation (between brackets).

Table 3

.

OTU nr	Identification [a]	Abundance (%)	Accession nr	H (%)	Source
1	*Longilinea*	30.31	JQ155218	99	Undefined full-scale anaerobic digester
2	*Leptolinea*	7.97	JQ104843	95	Undefined full-scale anaerobic digester
3	*Bacteroides*	7.67	GQ134121	99	Mesophilic anaerobic SBR treating swine waste (4.9 g N-TAN L^{-1})
6	*Levilinea saccharolytica*	1.15	EU407212	99	Household anaerobic digester
7	*Clostridium*	3.31	GQ995170	96	Mesophilic lab-scale anaerobic digester treating food industrial waste
12	*Acetivibrio*	1.45	GQ995163	99	Mesophilic lab-scale reactor treating food industrial waste
16	*Clostridium*	1.71	LN849648	99	Mesophilic lab-scale anaerobic digester reactor treating poultry manure
17	*Acholeplasma*	1.00	JN998160	99	Ammonium-stressed lab scale anaerobic digester
18	*Synergistes*	2.03	GQ134214	92	Mesophilic anaerobic SBR treating swine waste (1.0 g N-TAN L^{-1})
22	*Sterolibacterium denitrificans*	2.06	HM149064	92	Microbial fuel cell treating dairy wastewater
23	*Longilinea*	1.18	JQ104456	99	Undefined full-scale anaerobic digester
31	*Clostridium*	1.14	GQ136858	99	Mesophilic anaerobic SBR treating swine waste (5.2 g N-TAN L^{-1})
36	*Bacillus*	1.62	HQ183753	99	Undefined leachate sediment
2873	*Longilinea*	1.63	CU922827	98	Mesophilic anaerobic digester treating municipal wastewater sludge

[a] According to the GreenGenes database.

Figure 1

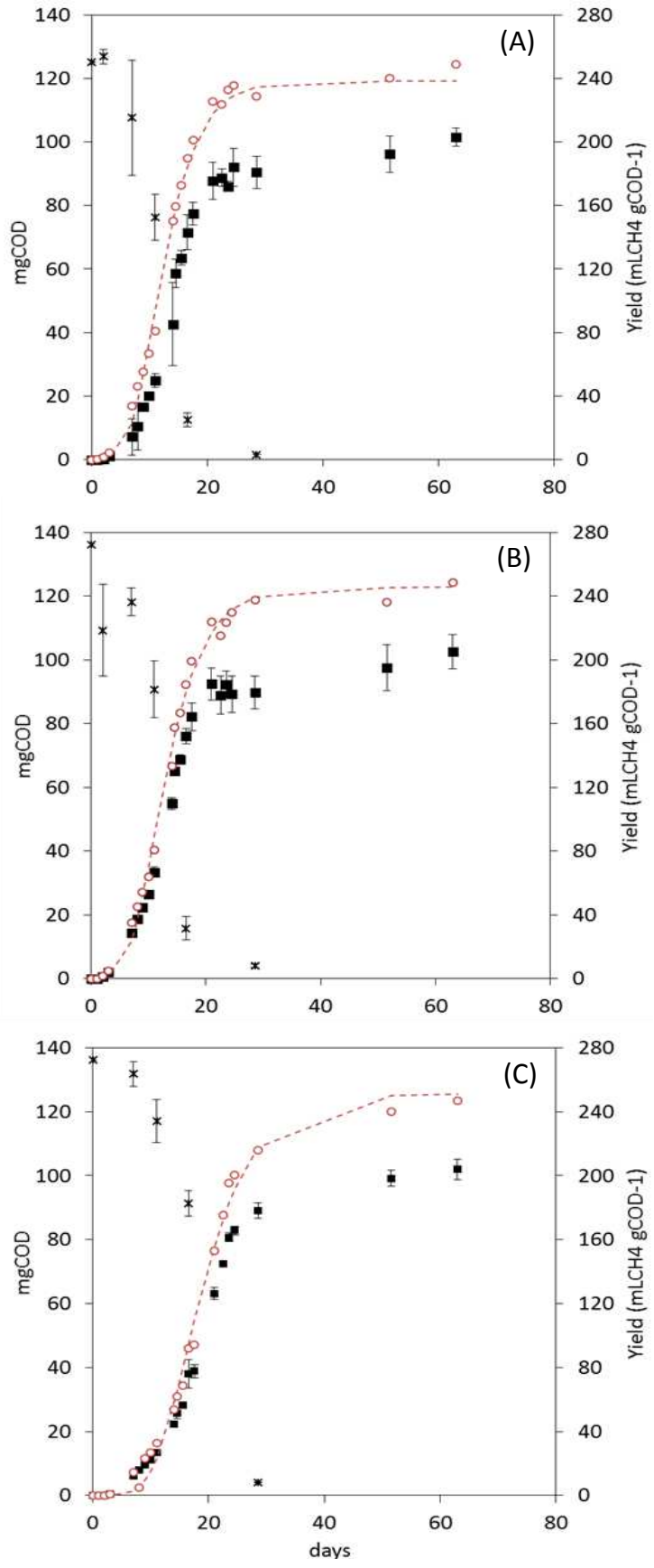
(A)
(B)
(C)
mgCOD
Yield (mLCH4 gCOD-1)
days
0
20
40
60
80
0
40
80
120
160
200
240
280
0
20
40
60
80
100
120
140

Figure 2

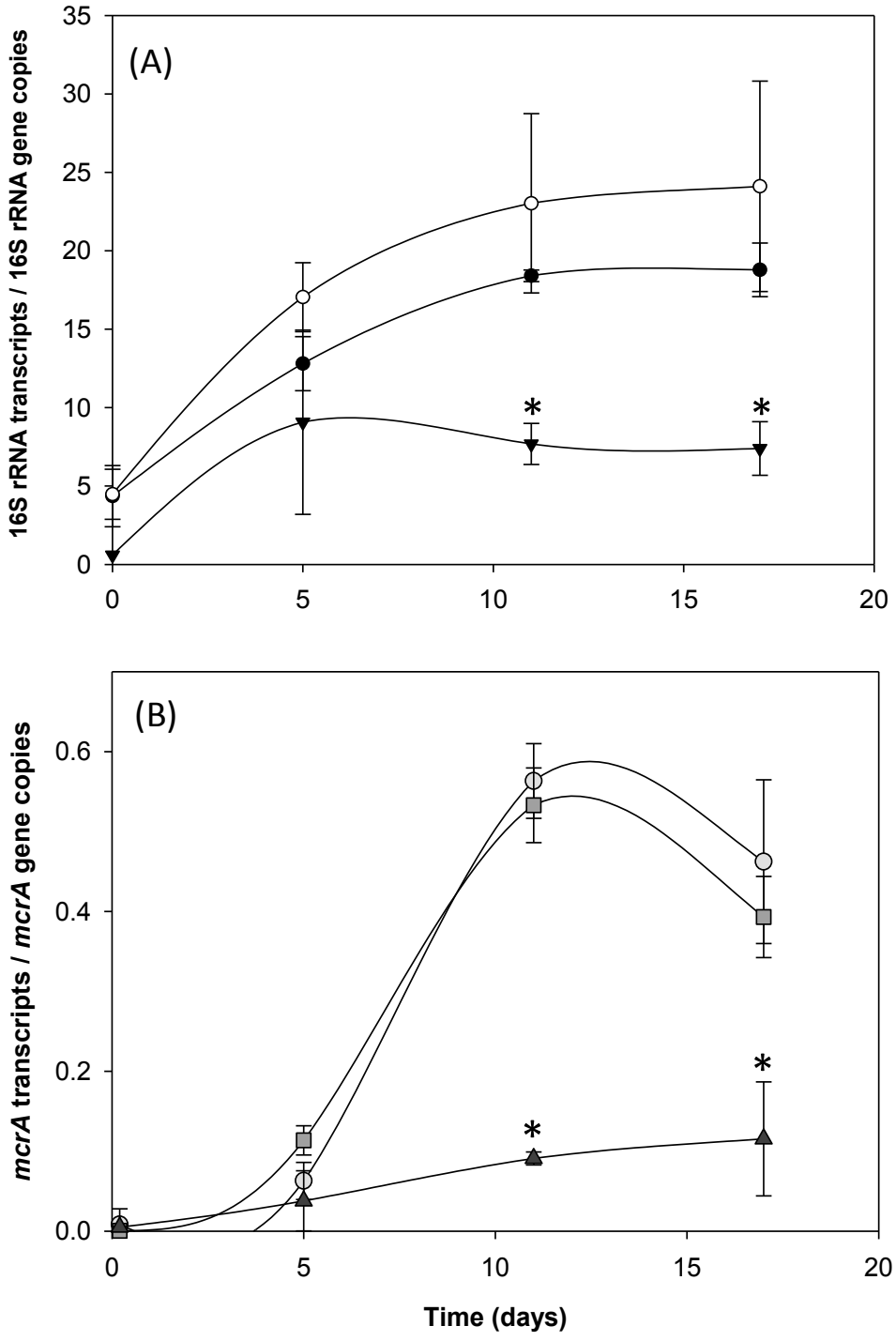
(A)
16S rRNA transcripts / 16S rRNA gene copies
35
30
25
20
15
10
5
0
0
5
10
15
20
*
*
(B)
mcrA transcripts / mcrA gene copies
0.6
0.4
0.2
0.0
0
5
10
15
20
*
*
Time (days)

Figure 3

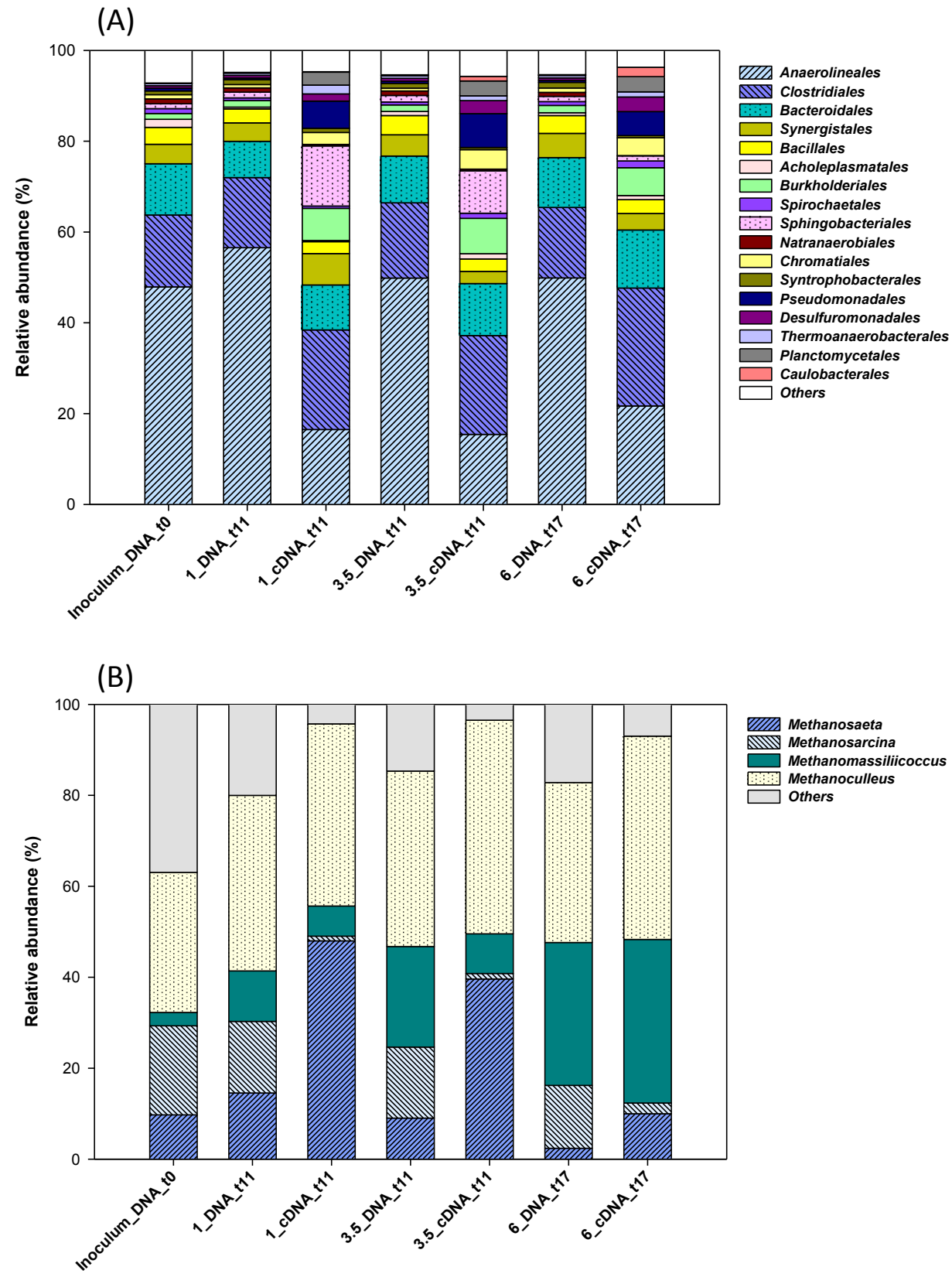
(A)
Relative abundance (%)
100
80
60
40
20
0
Inoculum_DNA_t0
1_DNA_t11
1_cDNA_t11
3.5_DNA_t11
3.5_cDNA_t11
6_DNA_t17
6_cDNA_t17
Anaerolineales
Clostridiales
Bacteroidales
Synergistales
Bacillales
Acholeplasmatales
Burkholderiales
Spirochaetales
Sphingobacteriales
Natranaerobiales
Chromatiales
Syntrophobacterales
Pseudomonadales
Desulfuromonadales
Thermoanaerobacterales
Planctomycetales
Caulobacterales
Others
(B)
Relative abundance (%)
100
80
60
40
20
0
Inoculum_DNA_t0
1_DNA_t11
1_cDNA_t11
3.5_DNA_t11
3.5_cDNA_t11
6_DNA_t17
6_cDNA_t17
Methanosaeta
Methanosarcina
Methanomassiliicoccus
Methanoculleus
Others

Figure 4

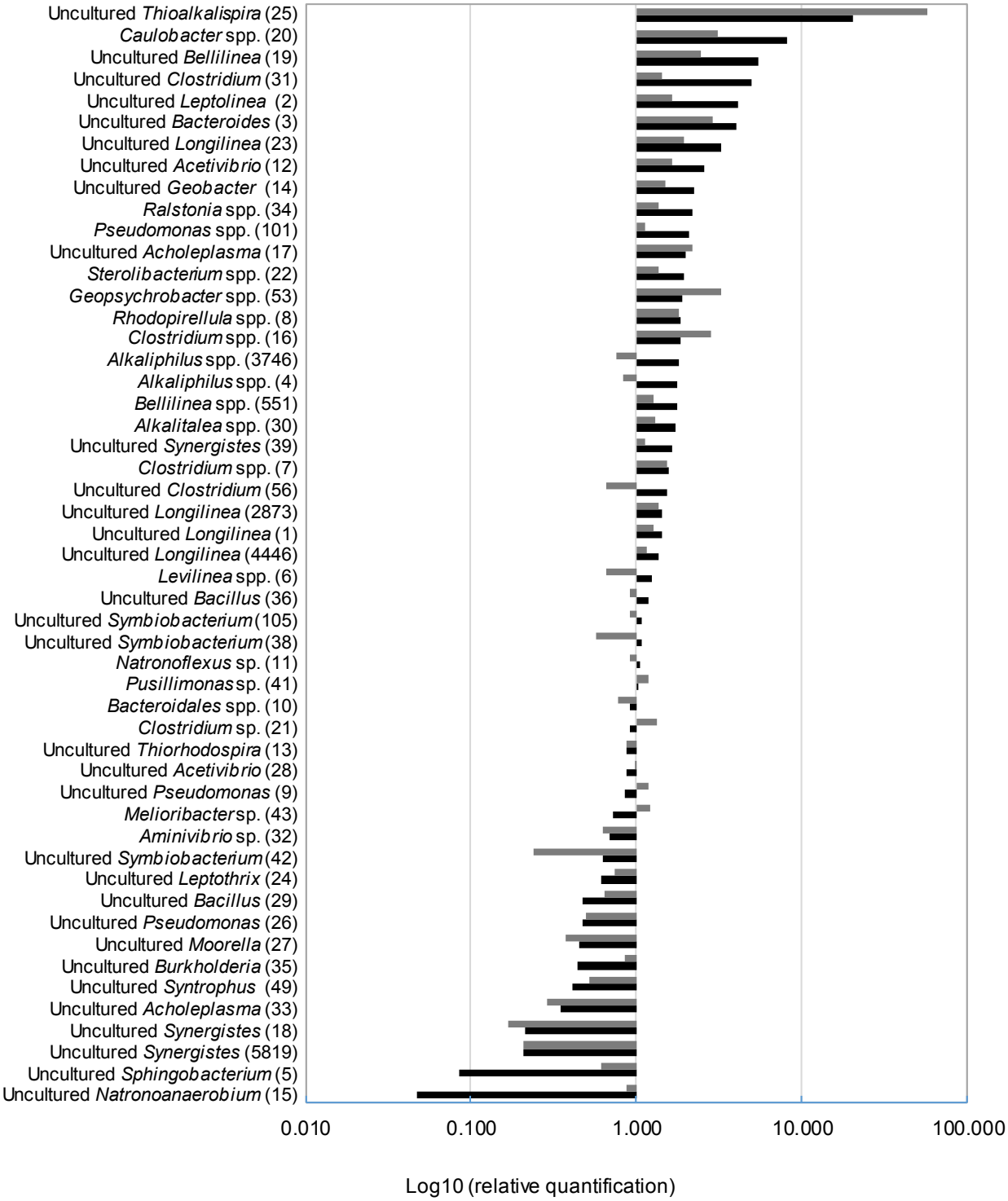
Uncultured *Thioalkalispira* (25)
Caulobacter spp. (20)
Uncultured *Bellilinea* (19)
Uncultured *Clostridium* (31)
Uncultured *Leptolinea* (2)
Uncultured *Bacteroides* (3)
Uncultured *Longilinea* (23)
Uncultured *Acetivibrio* (12)
Uncultured *Geobacter* (14)
Ralstonia spp. (34)
Pseudomonas spp. (101)
Uncultured *Acholeplasma* (17)
Sterolibacterium spp. (22)
Geopsychrobacter spp. (53)
Rhodopirellula spp. (8)
Clostridium spp. (16)
Alkaliphilus spp. (3746)
Alkaliphilus spp. (4)
Bellilinea spp. (551)
Alkalitalea spp. (30)
Uncultured *Synergistes* (39)
Clostridium spp. (7)
Uncultured *Clostridium* (56)
Uncultured *Longilinea* (2873)
Uncultured *Longilinea* (1)
Uncultured *Longilinea* (4446)
Levilinea spp. (6)
Uncultured *Bacillus* (36)
Uncultured *Symbiobacterium* (105)
Uncultured *Symbiobacterium* (38)
Natronoflexus sp. (11)
Pusillimonas sp. (41)
Bacteroidales spp. (10)
Clostridium sp. (21)
Uncultured *Thiorhodospira* (13)
Uncultured *Acetivibrio* (28)
Uncultured *Pseudomonas* (9)
Melioribacter sp. (43)
Aminivibrio sp. (32)
Uncultured *Symbiobacterium* (42)
Uncultured *Leptothrix* (24)
Uncultured *Bacillus* (29)
Uncultured *Pseudomonas* (26)
Uncultured *Moorella* (27)
Uncultured *Burkholderia* (35)
Uncultured *Syntrophus* (49)
Uncultured *Acholeplasma* (33)
Uncultured *Synergistes* (18)
Uncultured *Synergistes* (5819)
Uncultured *Sphingobacterium* (5)
Uncultured *Natronoanaerobium* (15)
0.010
0.100
1.000
10.000
100.000
Log10 (relative quantification)

*Graphical Abstract

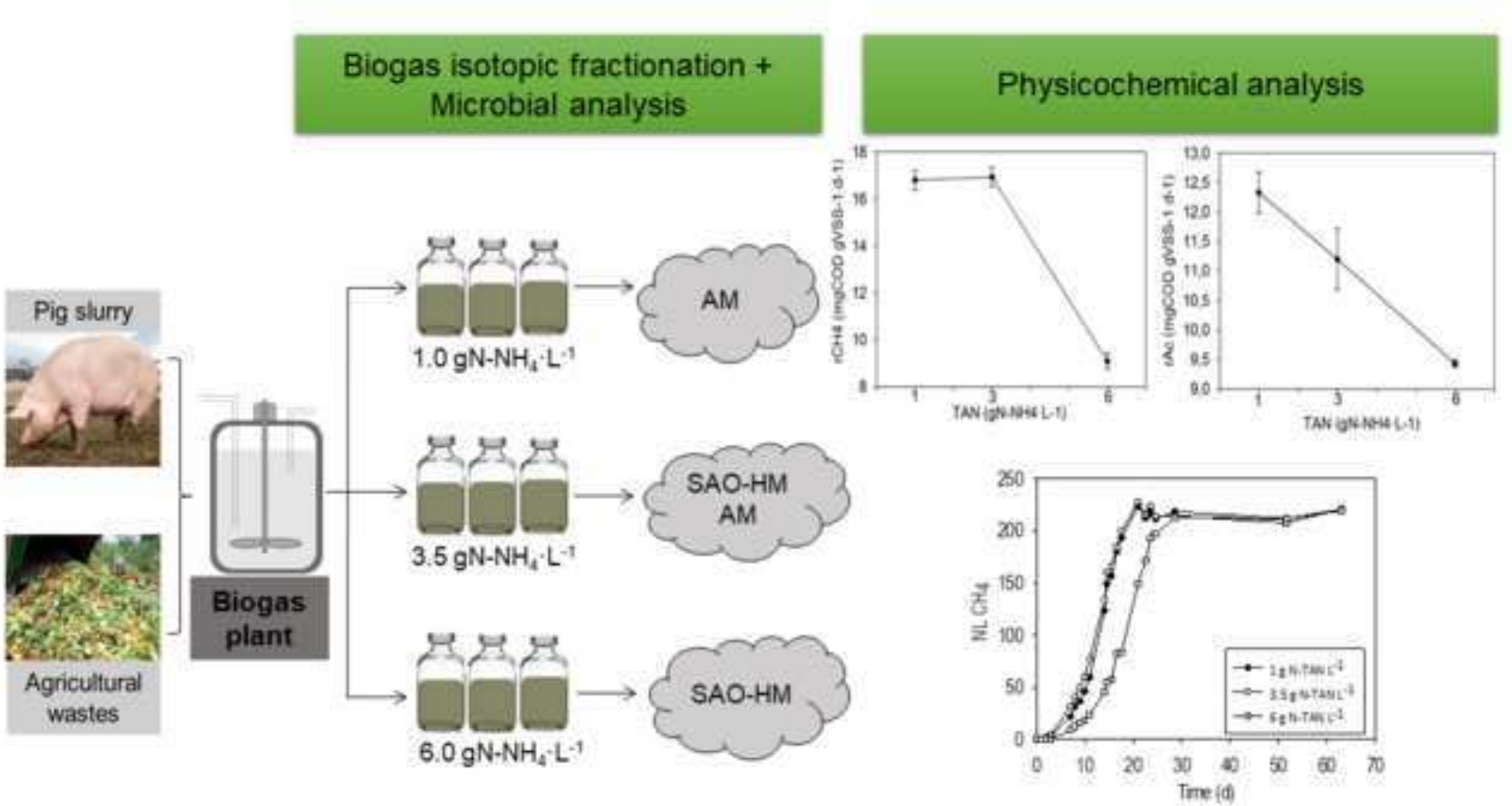

*AM: Acetotrophic methanogenesis / HM: Hydrogenotrophic methanogenesis/ SAO: Syntrophic acetate oxidation

***Highlights (for review : 3 to 5 bullet points (maximum 85 characters including spaces per bullet point)**

- N-adaptation of biomass in a full-scale digester ensued robust reactor performance
- NH_3 quickly shifted metabolism from acetotrophic to hydrogenotrophic methanogenesis
- Gene expression in several syntrophic bacteria was stimulated under high NH_3 exposure
- A novel archaeal *Methanoculleus* / *Methanomassiliicoccus* syntrophism is proposed
- The functional biodiversity of the SAO process still remains rather unexplored

Functional biodiversity and plasticity of methanogenic biomass from a full-scale mesophilic anaerobic digester treating nitrogen-rich agricultural wastes

J.Ruiz-Sánchez[1a], M. Guivernau[1a], B. Fernández[1], J. Vila[1, 2], M. Viñas[1], V. Riau[1], F.X. Prenafeta-Boldú[1,*]

[1] GIRO, Institute of Agrifood Research and Technology (IRTA), Torre Marimon, E08140 Caldes de Montbui, Barcelona, Catalonia, Spain.

[2] Department of Microbiology, University of Barcelona, UB. Av. Diagonal, 643, E08028, Barcelona, Catalonia, Spain.

*Corresponding author: francesc.prenafeta@irta.cat

[a]Both authors contributed equally to this manuscript.

Abstract

The effect of ammonia on methanogenic biomass from a full-scale agricultural digester treating nitrogen-rich materials was characterized in batch activity assays subjected to increasing concentrations of total ammonia N. Acetotrophic and methanogenic profiles displayed prolonged lag phases and reduced specific activity rates at 6.0 gN-TAN L^{-1}, though identical methane yields were ultimately reached. These results agreed with the expression levels of selected genes from bacteria and methanogenic archaea (qPCR of *16S* rRNA and *mrc*A cDNA transcripts). Compound-specific isotope analysis of biogas indicated that ammonia exposure was associated to a transition in methanogenic activity from acetotrophy at 1.0 gN-TAN L^{-1} to intermediate and complete hydrogenotrophy at 3.5 and 6.0 gN-TAN L^{-1}. Such pattern matched the results of 16S-Illumina sequencing of genes and transcripts in that predominant methanogens shifted, along with increasing ammonia, from the obligate acetotroph *Methanosaeta* to the hydrogenotrophic *Methanoculleus* and the poorly understood methylotrophic *Methanomassiliicoccus*. The underlying bacterial community structure remained rather stable but, at 6.0 gN-TAN L^{-1}, the expression level increased considerably for a number of ribotypes that are related to potentially syntrophic genera (e.g. *Clostridium*, *Bellilinea*, *Longilinea*, and *Bacteroides*). The predominance of hydrogenotrophy at high ammonia levels clearly points to the occurrence of the syntrophic acetate oxidation (SAO), but known SAO bacteria were only found in very low numbers. The potential role of the identified bacterial and archaeal taxa with a view on SAO and on stability of the anaerobic digestion process under ammonia stress has been discussed.

Keywords: Ammonia; anaerobic-digestion; active microbiome; C-isotopic biogas fractionation; syntrophic-acetate-oxidation (SAO).

INTRODUCTION

The anaerobic digestion (AD) of organic materials is a well-consolidated technology for the treatment and revalorization of organic waste into renewable energy (methane from biogas), and contributes significantly to the sustainability of several industrial processes (Lettinga, 2010). However, a significant proportion of the organic waste generated by the agrifood sector contains relatively large amounts of nitrogenated compounds (i.e. animal dejections, slaughterhouse by-products, and other protein-rich food-processing wastes). Organic nitrogen compounds are reduced to free ammonia (NH_3), often referred as free ammonia N (FAN), and its ionized counterpart ammonium (NH_4^+). In aqueous media, these two chemical species are in a pH and temperature-depending equilibrium. NH_3 is by far a stronger inhibitor of methanogenesis than NH_4^+ but, because of practical reasons, NH_3 and NH_4^+ are commonly measured together as total ammonia N (TAN) (Yenigün and Demirel, 2013). Such inhibitory effects might affect all microbial communities involved in the AD syntrophy, but the methanogenic archaea appear to be particularly sensitive to ammonia exposure (Demirel and Scherer, 2008). Yet, not all methanogens are affected equally; acetoclastic methanogenic archaea (AMA), which under common non-inhibitory conditions are responsible for most of the generated methane (CH_4), have been described to be vulnerable to relatively low concentrations of ammonia (circa 3.5 gN-TAN L^{-1}) (Banks et al., 2012; Schnürer and Nordberg, 2008). Conversely, the less sensitive hydrogenotrophic methanogenic archaea (HMA) are able to remain active at those concentrations, while reported ammonia inhibition thresholds are above 5 gN-TAN L^{-1} (Wang et al., 2015). Furthermore, AMA inhibition by ammonia might result in the accumulation of acetate up to inhibitory levels, thus contributing further to a negative feedback mechanism that eventually leads to complete reactor failure (Wang et al., 2015).

65 Under such high concentrations of ammonia and/or acetate, the so-called syntrophic
66 acetate oxidizing bacteria (SAOB) are able to reverse the homoacetogenic pathway and
67 convert acetate to carbon dioxide (CO_2) and hydrogen (H_2) (Schnürer et al., 1999). This
68 process is thermodynamically favourable through the concomitant consumption of H_2 by
69 HMA and, therefore, the syntrophic association between SAOB and HMA prevents the
70 inhibition of methanogenesis during the AD of nitrogen-rich substrates (Petersen and
71 Ahring, 1991). An increasing number of SAOB strains have been isolated in the recent
72 years and their physiology and genetics have been characterized quite thoroughly, but
73 information on the diversity, occurrence and role of SAOB in full-scale anaerobic digesters
74 is still limited (Westerholm et al., 2016). In an earlier integrative study based on the
75 metagenomic characterization of biomass and on the biogas isotopic profiling of different
76 industrial anaerobic digesters, we pointed out at the predominance of both HMA
77 communities and the hydrogenotrophic pathway in those digesters operated under
78 relatively high nitrogen loads (Ruiz-Sánchez et al., 2018). These conditions are conducive
79 to the enrichment of SAOB.

80 Here we aim at gaining a deeper insight into the microbial interactions, both of
81 metabolically active bacterial and archaeal populations that are potentially involved in the
82 SAO process. This new study focuses at the methanogenic biomass from an industrial
83 anaerobic digester treating nitrogen-rich agricultural wastes with no previous records of
84 process inhibition. A diversified research approach has been adopted for this purpose,
85 which combined batch methanogenic activity assays under different ammonia contents,
86 with Compound-Specific Isotope Analysis (CSIA) of $^{13}C/^{12}C$ natural isotopic fractionation of
87 CH_4 and CO_2 in the generated biogas, and the in-depth characterization of present and
88 metabolically active microbial populations by 16S-Illumina sequencing. The time-course

89 expression of relevant genes from bacteria (*16S* rRNA) and methanogenic archaea
90 (methyl coenzyme M reductase; *mcr*A) was quantified by qPCR.

91 MATERIALS AND METHODS

92 Batch experiments

93 Methanogenic biomass was collected from a 1,500 m^3 full-scale completely stirred tank
94 reactor (CSTR) for the anaerobic co-digestion of pig slurry and protein-rich agricultural
95 wastes (Vilasana, Lleida, Spain). This digester was operated according to the following
96 average parameters: total ammonia N (TAN) = 5.2 gN-TAN L^{-1}, chemical oxygen demand
97 (COD) = 101.2 gO_2 L^{-1}, volatile suspended solids (VSS) = 61.2 g L^{-1}, pH = 8.3, acetate
98 concentration = 0.0 gAc L^{-1}, hydraulic retention time (HRT) = 65 days, and temperature
99 within the mesophilic regime. Experiments were conducted in triplicate batch cultures (120
100 mL total volume, 60 mL working volume, inoculated with 12.7 gVSS L^{-1}), containing 1.0,
101 3.5 or 6.0 gN-TAN L^{-1} by adding NH_4Cl and 2.36 gAc L^{-1} as sodium acetate. Anaerobic
102 conditions were generated by flushing N_2 during 10 min. Cultures were incubated at 37^{0}C
103 under rotatory shaking and a bicarbonate buffer solution was added to maintain a constant
104 pH of 8 throughout the experiment. Control vials with neither acetate nor ammonia were
105 included to assess the endogenous CH_4 production of the inoculum.

106 Specific rates of acetate consumption and CH_4 production were determined and
107 expressed as gCOD $gVSS^{-1}$ d^{-1} (conversion factors: 2.857 mgCOD $mLCH_4^{-1}$; 1.067 gCOD
108 gAc^{-1}). For this purpose, samples of the liquid phase from each batch replicate (1 mL)
109 were collected after 0, 7, 11 and 17 days of incubation and directly centrifuged (4ºC,
110 20,000 rpm, 5 minutes). The supernatant (clarified fraction) was used for chemical
111 analysis, while the pellets (sedimented fraction) were kept at -80ºC until further processing
112 via molecular biology tools. Samples from the headspace of each culture were taken

periodically for the characterization of the biogas composition during the experiment. CH_4 yield ($mLCH_4\ gCOD^{-1}$), lag phase and specific CH_4 production rate (rCH_4; $mgCOD\ gVSS^{-1}\ d^{-1}$) were calculated after fitting the experimental data to the modified Gompertz equation. Samples of the accumulated biogas at the end of the incubation were collected for analysing the natural $^{13}C/^{12}C$ isotopic fractionation of CH_4 and CO_2. Gas/liquid volume changes due to sampling were taken into account in the calculation of mass balances.

Analytical methods

Total Kjeldhal Nitrogen (TKN), TAN and pH were determined according to the Standard Methods (APHA, 2005). The biogas was monitored along the experiment by sampling 100µl from headspace of each batch. Biogas composition (CH_4 and CO_2) and the concentration of individual volatile fatty acids (VFA) in the liquid media, including acetic (Ac), propionic, butyric, valeric and caproic acids, were measured in a gas chromatograph (Varian CP-3800). This instrument was equipped with a Varian Hayesep-Q 80-100 mesh capillary column and a TCD detector for the analysis of biogas, or a TRB-FFAP capillary column and a FID detector for the analysis of VFA.

CSIA of $^{13}C/^{12}C$ natural isotopic fractionation of biogas components was carried out by gas chromatography combustion–isotope ratio mass spectrometry (GC–IRMS). An Agilent 6890 gas chromatograph was fitted with a split/splitless injector and coupled to an isotope ratio mass spectrometer (Delta Plus Finnigan MAT) via a combustion interface (850°C), consisting of a 60 cm quartz tube (0.65 mm ID) filled with copper oxide. A liquid nitrogen cold trap was used to remove water. Separation was achieved on a CpsilCB (Chrompack) fused silica capillary column (60 m×0.32 mm; 0.12 µm film thickness) using He as carrier gas. The oven temperature was held at 40°C for 1 min, and increased to 320°C at a rate of 10°C min^{-1}. This final temperature was maintained for 25 minutes.

Squalene was used as internal standard. Each sample was run in triplicate to ensure reproducibility within ±0.2‰ (1σ), relative to the Vienna Pee Dee Belemnite (VPDB) standard. All carbon isotopic ratios were expressed as ‰ relative to the VPDB standard, and the apparent fractionation factor (αC) was determined according to Conrad et al., (2009). A αC within the range of 1.040 – 1.055 corresponded to a predominantly acetotrophic AD process, while that of 1.055 – 1.080 was mainly hydrogenotrophic (Conrad, 2005; Penning and Conrad, 2007).

Molecular methods

Total genomic DNA and RNA from all previously centrifuged biomass samples (pellets) were simultaneously extracted by an adapted protocol of the PowerMicrobiome™RNA Isolation kit (Qiagen). The RNA extracts were treated during 10 min at 25 °C with 10 units of DNase I to remove any contamination of genomic DNA, and directly subjected to a 16S rRNA-based PCR amplification to verify their purity (Prenafeta-Boldú et al., 2014). RNA extracts were subsequently transcribed to cDNA by means of PrimeScript™ RT reagent Kit (Perfect Real Time, Takara) following the manufacturer's instructions. cDNA and DNA extracts were kept frozen at −80 °C until further analysis.

Total and active bacterial populations and methanogenic archaea were quantified by means of qPCR amplification of *16S* rRNA and *mcrA* genes, respectively (Sotres et al., 2014). Reactions were carried out using the Brilliant II SYBR Green qPCR Master Mix (Stratagene) on a Real-Time PCR System Mx3000P (Stratagene). The specificity of the qPCR amplifications was determined by observations of the corresponding melting curves and gel electrophoresis profiles. To prepare the corresponding standard curves two duplex DNA were synthesized (Metabion GmbH). Ten-fold serial dilutions of both standard genes

were subjected to qPCR assays in duplicate showing a linear response between 10^1 and 10^8 gene copy numbers. The qPCR standards for both genes fitted quality standards with amplification efficiencies between 90 and 110% and R^2 above 0.985. All results were processed by the MxPro™ QPCR software (Stratagene). All results obtained from triplicate independent batches were treated statistically. The Shapiro-Wilk test was performed to determine whether data were normally distributed. Considering the paired structure and normal distribution of the data, an analysis of variance (ANOVA) was performed. The combination of factors were the sampling time (0, 7, 11 and 17 days) and the TAN treatments (1.0, 3.5 and 6.0 gN-TAN). Subsequently, pairwise comparisons Fisher's least significant difference (LSD) were applied to test differences between batches by sampling periods. The significance threshold was established at 0.05 type I error. All statistical analysis were performed by means of XLSTAT 2018 software (Addinsoft) and SigmaPlot 11.0 software.

The time course evolution of methanogenic activity and expression of 16S rRNA and *mcrA* genes determined the sampling periods for high throughput sequencing. The microbial community structure was characterized by 16S-Illumina sequencing analysis after 11 and 17 days, respectively for batches exposed to 1.0, 3.5, and 6.0 gN-TAN L^{-1}, when the maximum CH_4 production rates and gene expression level was recorded (Figures 1 and 2). Microbial diversity in the bacteria and archaea domains was assessed in duplicate by means of *16S* rRNA Illumina (MiSeq) high-throughput sequencing as described previously (Pelissari et al., 2017). The obtained DNA and cDNA reads were compiled in FASTq files for further bioinformatic processing. Trimming of the 16S rRNA barcoded sequences into libraries was carried out using the QIIME software version 1.8.0 and quality filtering of the reads was performed at Q25, prior to their grouping into Operational Taxonomic Units (OTUs) at a 97% sequence homology cut-off. OTUs were then taxonomically classified

using the RDP Naïve Bayesian Classifier (2.2) with a bootstrap cut-off value of 80%, and compiled to each taxonomic level.

The number of observed OTUs, Goods coverage, alpha biodiversity parameters (the inverted Simpson and Shannon indexes), and species richness (Chao1 estimator) were calculated using the Mothur software v.1.35.9 (http://www.mothur.org). The number of reads were rarefacted to the lowest number among the different samples. The sequence data from the MiSeq NGS assessment were submitted to the Sequence Read Archive (SRA) of the National Center for Biotechnology Information (NCBI) under the study accession number PRJNA385091.

RESULTS AND DISCUSSION

Batch incubation experiments

Methanogenic activity assays

The time-course evolution of acetate and CH_4 was monitored at low, intermediate and high ammonia exposure (1.0, 3.5, and 6.0 gN-TAN L^{-1}) in batches that were inoculated with freshly collected biomass from the studied agricultural anaerobic digester (Figure 1). The estimated FAN concentrations at the tested intermediate and high ammonia exposure were above the inhibitory threshold for methanogenesis (Table 1), considering that values as low as 250 mg L^{-1} have been found to impair the anaerobic digestion process with unaclimated biomass (Yenigün and Demirel, 2013). The specific acetate uptake rate (*r*Ac) was similar up to 3.5 gN-TAN L^{-1} but it decreased by 46% at 6.0 gN-TAN L^{-1} (Table 1). The impact of ammonia on methanogenesis was also significant since the CH_4 production rate (rCH_4) decreased by 26% and 31% upon ammonia exposure at 3.5 and 6.0 gN-TAN L^{-1}, with respect to the rCH_4 at 1 gN-TAN L^{-1} (Table 1). This apparent ~~higher~~ vulnerability of acetate-utilizing microorganisms might be the result of the well-known susceptibility of

AMA to ammonia (Hunik et al., 1990). Under such conditions, acetate might also be consumed by the SAOB but this metabolic process has been associated to relatively low conversion rates (Sun et al., 2014). Along with a high ammonia content, those digesters were often characterized by a prolonged biomass retention time and thermophilic temperature, parameters that have been identified as crucial for the enrichment of the rather slow-growing SAO microbial communities (Sun et al., 2014). However, despite the lower metabolic rates under high ammonia concentrations, all tested batches reached a similar CH_4 yield and more than the 80% of the added acetate was eventually recovered as CH_4 in terms of COD equivalents.

Isotopic fractionation of biogas

Most of the previous studies on the application of isotopic analysis of biogas for the characterization of anaerobic digesters subjected to high ammonia levels were based on using radioactive (Karakashev et al., 2006; Sun et al., 2014) or stable (Mulat et al., 2014) isotope-labelling at the acetate methyl group. The protocol implemented in this study based on CSIA of $^{13}C/^{12}C$ natural isotopic fractionation provided a deeper insight on the methanogenic pathways, without the need of using expensive and/or dangerous labelled substrates. The apparent fractionation factor α_C as defined by Whiticar and Faber (1986) from the measured δCH_4 and δCO_2, and later reviewed by (Conrad et al., 2009) was used. This factor indicates that environments with a $\alpha_C<1.055$ are dominated by AMA, while those with a $\alpha_C>1.065$ point to the predominance of HMA (up to exclusive hydrogenotrophy at $\alpha_C=1.085$). From the α_C values calculated in the present study, it can be concluded that increasing the ammonia content prompted a metabolic shift in methanogenesis from AMA at 1.0 gN-TAN L^{-1} to a HMA activity that was predominant at 3.5 gN-TAN L^{-1}, and even exclusive at 6.0 gN-TAN L^{-1} (Table 1). This shift from acetotrophic to hydrogenotrophic methanogenesis is consistent with previous observations

from anaerobic digesters under increasing ammonia concentrations (Wang et al., 2015). Concurrent prevalence of hydrogenotrophy along with consumption of acetate (added as the sole electron source), strongly supports the hypothesis that biomass from the studied anaerobic digester contained SAO species that were active under a relatively high ammonia content. Furthermore, these results also indicate that, despite its previous history of acclimation and adaptation to high nitrogen loads, the methanogenic biomass was still able to modulate the metabolism towards acetotrophy when exposed to low concentrations of ammonia.

Microbial community analysis

Quantitative expression profile of selected functional genes

The effect of ammonia on the expression ratio (qPCR quantification of transcripts versus gene copies) of specific functional genes from bacteria (*16S* rRNA) and methanogenic archaea (*mcr*A) was consistent with the previously observed profiles of acetate consumption and CH_4 generation (Figure 1). The bacterial *16S* rRNA expression ratio increased in time, reaching a maximum value at around day 11 that was maintained until the end of incubations at day 17 (Figure 2a). This maximum expression ratio was a 53% lower at 6.0 gN-TAN L^{-1}, in relation to that of 1.0 gN-TAN L^{-1} (differences between 1.0 and 3.5 gN-TAN L^{-1} were not significant). Despite the fact that the expression of ribosomal genes must be regarded as a global metabolic indicator for all bacteria, and so it cannot univocally be associated to the acetotrophic activity, it might partly explain the reduction in *r*Ac that occurred at high ammonia concentrations (Table 1).

For the archaea, instead, a much more specific gene directly related to methanogenesis was targeted. The expression ratio of *mcr*A genes at low and intermediate ammonia concentrations (1.0 – 3.5 gN-TAN L^{-1}) was very similar (Figure 2b). The observed values

were rather low during the first 5 days of incubation but they sharply peaked at around day 11, to decrease again at day 17. Such unimodal profile fits the observed lag-phase in CH_4 production of approximately 6 days and the exponential phase in CH_4 accumulation that followed, before the declining phase that started shortly after day 11. Incubations with the highest ammonia concentration (6.0 gN-TAN L^{-1}) resulted in a *mcr*A expression ratio that was a 83% lower than those at low and intermediate ammonia exposure (Figure 2b). As discussed previously, these batches showed the longest lag-phases and the lowest *r*CH_4 production, but similar CH_4 yields were eventually achieved.

Bacterial community structure and response to ammonia exposure

The microbial community structure from the most active period during the batch activity assays was assessed by high throughput DNA sequencing. A total of 440,756 and 224,133 high quality *16S* rRNA ribosomal genes and transcripts (cDNA) reads were obtained for the *Bacteria* domain. These reads were grouped into operational taxonomic units (OTUs, defined at 97% sequence homology cut-off) and confidently assigned to specific taxa (Table 2). The Good's coverage estimator on the percentage of the total species (as OTUs) represented at any given sample was above 99%, indicating that the observed bacterial species encompassed most of the samples' populations. Species biodiversity (Shannon and inverted Simpson indexes) and richness (Chao1) were rather similar among samples, with an estimated number of species in the inoculum of 5,592. Species richness in active bacterial populations (cDNA ribotype libraries) was always lower than that corresponding to the present species (DNA ribotype libraries), but the biodiversity of the active population increased upon ammonia exposure. This indicates that an important proportion of the species from the inoculum were metabolically active under the tested conditions, and that ammonia triggered the response of an increasingly complex bacterial community.

The bacterial community structure, based on 16S rRNA gene counts, remained relatively stable during all assays regardless of the TAN concentration (Figure 3a). Representatives of the order *Anaerolineales* were predominant, with a relative gene abundance (RGA) of more than 40% in all assays. Other important groups included members of the orders *Clostridiales* (16% RGA) and *Bacteroidales* (9–12% RGA), the former being particularly relevant as it encompasses most of the recently described SAOB. In our previous metagenomic study (Ruiz-Sánchez et al., 2018) we suggested that members of phyla *Bacteroidetes*, along with *Chloroflexi*, might encompass yet undescribed SAOB.

In contrast with this stable microbial community structure, a population shift was observed in the active species when exposed to increasing ammonia concentrations. In terms of relative transcript abundance (RTA), members of the *Clostridiales* (22–26% RTA) and *Anaerolineales* (14–20% RTA) were among the most active communities. Other relevant metabolically active groups were found in the *Bacteroidales* (9–12% RTA), *Burkholderiales* (5–8% RTA), *Pseudomonadales* (5–7% RTA) and *Planctomycetales* (3% RTA). In contrast to these groups, which displayed little sensitivity to ammonia, *Sphingobacteriales* showed a clear negative correlation with the concentration of ammonia, so that their RTA decreased from 15% to 1% upon an ammonia supplementation from 1.0 to 6.0 gN-TAN L^{-1}.

The high throughput sequencing data from this study was also mined for the presence of well-known SAOB (Fotidis et al., 2013). OTUs homologous to the thermotolerant/thermophilic *Tepidanaerobacter acetatoxydans* and *Thermacetogenium phaeum* were detected, but in very low abundance and only in certain samples. Therefore, these particular thermophilic species played a minor role in the studied mesophilic reactor. Nevertheless, the proven hydrogenotrophy at relatively high TAN levels and the absence

308 of acetate accumulation, suggested that other non-described mesophilic SAO microbial
309 communities must be active in the biomass.

310 The *16S* rRNA gene expression ratio (transcripts to genes) at intermediate and high
311 ammonia levels (3.5 and 6.0 gN-TAN L^{-1}), in relation to that of the basal concentration (1.0
312 gN-TAN L^{-1}) gives a further insight on the response of relevant bacterial species (as
313 OTUs) to ammonia exposure (Figure 4). The highest expression shift along with increasing
314 TAN concentrations was observed for a number of OTUs related to the genera
315 *Thioalkalispira*, *Caulobacter*, *Bellilinea*, *Clostridium*, *Leptolinea*, *Bacteroides* and
316 *Acetivibrio*; while representatives of the genera *Natronoanaerobium*, *Sphingobacterium*,
317 and *Synergistes* appeared to be inhibited at 6.0 gN-TAN L^{-1}. Individual BLAST searches
318 from the sequences of the "ammonia-philic" OTUs yielded uncultured bacteria from a
319 variety of anaerobic digesters that might have been exposed to relatively high ammonia
320 levels (Table 3). Of particular interest is OTU1, which appears to be somewhat related to
321 the genus *Longilinea* (94% sequence homology) and was by far the most abundant
322 ammonia-responding OTU (30% in RTA). The second most active species (OTU2, 8% in
323 RTA), also belonged to the class *Anaerolineae* (*Chloroflexi*), and displayed its highest
324 similarity to a member of the genus *Leptolinea* (88% sequence homology). Four additional
325 OTUs affiliated within the same class (genera *Levilinea* and *Bellilinea*) also increased their
326 relative activity in the presence of ammonia, but their abundance was significantly lower.
327 The class *Anaerolineae* was described in order to accommodate four new isolates
328 originating from mesophilic UASB reactors (*Levilinea saccharolytica* and *Leptolinea*
329 *tardivitalis*) (Yamada et al., 2006), a rice paddy soil (*Longilinea arvoryzae*), and a
330 thermophilic digester (*Bellilinea caldifistulae*) (Yamada et al., 2007). They have relatively
331 prolonged doubling times (45 – 92 h) and differ in their optimal temperature for growth,
332 which could explain the low occurrence of the thermophilic *Bellilinea* in the mesophilic

reactor. Interestingly, *Longilinea* and *Bellilinea* share the fact that growth is enhanced in co-cultivation with hydrogenotrophic methanogens. Nevertheless, neither H_2/CO_2 nor acetate served as sole carbon sources for growth in pure cultures, so that their potential role as SAOB might be put into question.

A ribotype distantly related to *Bacteroides* (OTU3) could also have played a relevant role in the anaerobic digestion of nitrogen-rich substrates, given its relatively high expression level (8% RA of ribosomal transcripts). Despite poor phylogenetic definition, OTU3 exhibits a relatively high sequence similarity to several uncultured bacteria from anaerobic digesters, including an anaerobic sequencing batch reactor (SBR) treating swine waste at 4.9 g N-TAN L^{-1} (Angenent et al., 2002). A number of unidentified clostridia (OTUs 7, 16, and 31) with a significant presence in the methanogenic biomass (>1%) increased their relative expression under high ammonia concentrations, and revealed high sequence similarity with ribotypes previously reported in other ammonia-rich anaerobic digesters. It could thus well be that some of the above mentioned OTUs correspond to yet undescribed SAOB.

Archaeal community structure and response to ammonia exposure

High throughput DNA sequencing of the *Archaea* yielded 401,486 genes and 444,516 transcript reads. As with the bacteria, the Good's coverage estimator for the archaea was above 99%, but the Chao1 estimator was one order of magnitude lower, with a predicted 414 archaeal species in the original inoculum. Both the biodiversity and number of active archaea were always lower than those corresponding to the present species (DNA ribotype libraries) so that, contrary on the bacteria, an increasing ammonia exposure generated a less diversified response of the archaeal community. The original methanogenic biomass (inoculum) was primarily composed by strict hydrogenotrophic

orders, such as *Methanomicrobiales* (*Methanoculleus*, 31% RGA) and *Methanobacteriales* (*Methanobrevibacter*, 26% RGA), but also the metabolically versatile *Methanosarcinales* (30% RGA), which encompasses both facultative and obligate acetotrophic genera (*Methanosarcina* and *Methanosaeta*). Representatives of the thermophilic chemolithoautotrophic ammonia oxidizing archaeon *Nitrosocaldus* were also present at a lower yet relevant abundance (7% RGA). Contrary to the bacteria, a significant population shift was observed for the archaea after incubations, in terms of gene counts (RGA), along with increasing ammonia concentrations. *Methanosaeta* decreased from 10% RGA at 1.0 gN-TAN L^{-1} to less than 3% at 6.0 gN-TAN L^{-1}, while representatives of *Methanomassiliicoccus* (order *Methanomassiliicoccales*) where enriched from 11% RGA (1.0 gN-TAN L^{-1}) up to 31% RGA (6.0 gN-TAN L^{-1}). This novel order of methyl-dependent hydrogenotrophic methanogens encompasses the former, recently reclassified, *Thermoplasmatales* (Adam et al., 2017; Borrel et al., 2014). Species from the *Methanomassiliicoccales* have recently been found in various anaerobic environments and are becoming an emerging research subject due to their scarcely known biology (Ziganshin et al., 2016).

The profiles of active archaea were rather similar at 1.0 and 3.5 gN-TAN L^{-1}, with *Methanosaeta* (48%–40% RTA) and *Methanoculleus*, (40%–47% RTA) as the most active genera (Figure 3b). *Methanoculleus* maintained a rather high level of gene expression regardless of ammonia exposure (about 45% RTA), but activity increased significantly for *Methanomassiliicoccus* (36% RTA) at 6.0 gN-TAN L^{-1}. This finding further confirms that hydrogenotrophy had become the predominant methanogenic process at a high ammonia content, as seen previously from the isotopic fractionation profiles (Table 1). Furthermore, the extraordinary growth and activity levels of *Methanomassiliicoccus* indicates that this

particular taxon plays a vital role in the anaerobic digestion process under the tested high ammonia conditions and, therefore, it deserves further attention.

Recent genomic evidence points out to a number of physiological and metabolic features of the *Methanomassiliicoccales* that are relevant for this study. To start with, this order is characterized by the presence of quaternary ammonium efflux pumps (Borrel et al., 2014), which might explain why it thrived under high ammonia concentrations. They also lack the methyl-branch of the archaeal type Wood–Ljungdahl pathway and the coenzyme M methyltransferase complex (MTR), which makes them reliant on methyl-dependent hydrogenotrophic methanogenesis (Adam et al., 2017). Interestingly, the *Methanomassiliicoccales* have the genetic capability of heterotrophic growth on acetate and, possibly, of synthesizing acetyl-CoA from formate and CO_2 (Lang et al., 2015). These findings are in agreement with metagenomic evidence that species in the *Methanomassiliccoccales* harbour several genes related to acetyl-CoA pathway (Campanaro et al., 2016). Species in this taxon might therefore be able to transform acetate to CO_2, but they also possesses the *fhd*A gene encoding a glutathione-dependent formaldehyde dehydrogenase that transform formaldehyde to formate. Additionally, a recent study on the evolution of the bifunctional enzyme acetyl-CoA synthase/carbon monoxide dehydrogenase gene cluster (ACS/CODH) claimed that the *Methanomassiliicoccales* have a bacterial-type CODH, likely due to ancient interdomain transfer events (Adam et al., 2018). The CODH enzymes are used by aerobic and anaerobic carboxytrophs to catalyze the reversible conversion between CO_2 and CO. Remarkably, in the *Methanomassiliicoccales*, these enzymes only function in the oxidative direction due to their inability of carbon fixation.

Hence, considering the relevance of the predominant OTUs affiliated to *Methanomassiliccocales* from the present study, an *in silico 16S* rRNA assessment with

406 different databases (RDP, GreenGenes and BLAST) was performed. As a result, the
407 affiliation of OTU4 to the *Methanomassiliicoccales*, and more specifically to the genus
408 *Methanomassiliicoccus*, was confirmed. We propose a novel archaeal syntrophic
409 association between species in the genus *Methanoculleus*, which have consistently been
410 reported to prevail in ammonia-enriched anaerobic digesters dominated by the SAO
411 process (Sun et al., 2014), and *Methanomassiliicoccus*. The latter would then acts as
412 archaeal SAO, analogue to the known SAOB, by converting acetate to formate and/or
413 CO_2, substrates that would then be consumed by *Methanoculleus*. The association
414 between *Methanomassiliicoccus* and *Methanoculleus* has already been reported in an
415 anaerobic digestor treating food waste, where their dominance was strongly correlated
416 with accumulation of VFA, increasing OLR, and concentration of ammonia (Li et al., 2018).

417 **CONCLUSIONS**

418 Biomass from a full-scale anaerobic digester adapted to relatively high ammonia
419 concentrations was able to swiftly change its metabolic mode from acetotrophic to
420 hydrogenotrophic methanogenesis upon increasing ammonia levels, by
421 activating/deactivating specific microbial populations. Biological activity was negatively
422 affected at the highest tested ammonia concentration (6.0 gN-TAN L^{-1}), both in terms of
423 CH_4 production and acetate consumption rates, as well as in relation to a decreasing
424 expression level of bacteria and methanogenic archaea, but a similar CH_4 yield was
425 eventually achieved with all tested nitrogen conditions.

426 In contrast to the bacterial community structure, which remained relatively stable during
427 the experiments, important changes for the active species were observed in response to
428 ammonia. Despite the strong evidence for the occurrence of the SAO process under high
429 ammonia concentrations, none of the SAOB that are currently known from the literature

430 played a significant role in the studied biomass. However, several bacteria belonging to
431 taxa that have previously been associated to acetate metabolism were stimulated upon
432 ammonia exposure. Concerning the methanogenic archaea, the strictly acetotrophic genus
433 *Methanosaeta* was among the most active under low ammonia concentrations (1.0 gN-
434 TAN L^{-1}). However, *Methanosaeta* quickly declined both in biomass abundance and in
435 activity at higher ammonia levels, and was overtaken by representatives of the
436 hydrogenotrophic genera *Methanoculleus* and *Methanomassiliicoccus*. Such archaeal
437 association could be explained by the extraordinary metabolic flexibility and
438 complementary of these two genera, which contribute to both acetotrophy and
439 hydrogenotrophy.

440 **Acknowledgements**

441 This work was supported by Spanish government under the INIA project *"PROGRAMO*
442 *Advanced anaerobic treatment of wastes with high lipid/protein content, with ammonia*
443 *recovery"* program no. (RTA2012-00098-00-00). The first author has a grant from Spanish
444 government (FPI-INIA RTA2012-00098-00-00). IRTA thanks the financial support of
445 CERCA program of the Generalitat de Catalunya.

446

447 **REFERENCES**

448 American Public Health Association (APHA) (2005) Standard method for examination of
449 water and wastewater, 21st edn. APHA, AWWA, WPCF, Washington
450 Adam PS, Borrel G, Brochier-Armanet C, Gribaldo S. 2017. The growing tree of Archaea:
451 New perspectives on their diversity, evolution and ecology. *ISME J.*
452 Adam PS, Borrel G, Gribaldo S. 2018. Evolutionary history of carbon monoxide
453 dehydrogenase/acetyl-CoA synthase, one of the oldest enzymatic complexes. *Proc.*

454 *Natl. Acad. Sci.*:201716667.
455 Angenent LT, Sung S, Raskin L. 2002. Methanogenic population dynamics during startup
456 of a full-scale anaerobic sequencing batch reactor treating swine waste. *Water Res.*
457 **36**:4648–4654.
458 Banks CJ, Zhang Y, Jiang Y, Heaven S. 2012. Trace element requirements for stable food
459 waste digestion at elevated ammonia concentrations. *Bioresour. Technol.* **104**:127–
460 135.
461 Borrel G, Parisot N, Harris HMB, Peyretaillade E, Gaci N, Tottey W, Bardot O, Raymann
462 K, Gribaldo S, Peyret P, O'Toole PW, Bruge`re JF. 2014. Comparative genomics
463 highlights the unique biology of Methanomassiliicoccales, a Thermoplasmatales-
464 related seventh order of methanogenic archaea that encodes pyrrolysine. *BMC*
465 *Genomics* **15**.
466 Campanaro S, Treu L, Kougias PG, De Francisci D, Valle G, Angelidaki I. 2016.
467 Metagenomic analysis and functional characterization of the biogas microbiome using
468 high throughput shotgun sequencing and a novel binning strategy. *Biotechnol.*
469 *Biofuels* **9**:26.
470 Conrad R. 2005. Quantification of methanogenic pathways using stable carbon isotopic
471 signatures: A review and a proposal. *Org. Geochem.* **36**:739–752.
472 Conrad R, Claus P, Casper P. 2009. Characterization of stable isotope fractionation during
473 methane production in the sediment of a eutrophic lake, Lake Dagow, Germany.
474 *Limnol. Oceanogr.* **54**:457–471.
475 Demirel B, Scherer P. 2008. The roles of acetotrophic and hydrogenotrophic methanogens
476 during anaerobic conversion of biomass to methane: A review. *Rev. Environ. Sci.*
477 *Biotechnol.* **7**:173–190.
478 Fotidis IA, Karakashev D, Angelidaki I. 2013. Bioaugmentation with an acetate-oxidising

consortium as a tool to tackle ammonia inhibition of anaerobic digestion. *Bioresour. Technol.* **146**:57–62.

Hunik JH, Hamelers HVM, Koster IW. 1990. Growth-rate inhibition of acetoclastic methanogens by ammonia and pH in poultry manure digestion. *Biol. Wastes* **32**:285–297.

Karakashev D, Batstone DJ, Trably E, Angelidaki I. 2006. Acetate oxidation is the dominant methanogenic pathway from acetate in the absence of Methanosaetaceae. *Appl. Environ. Microbiol.* **72**:5138–5141.

Lang K, Schuldes J, Klingl A, Poehlein A, Daniel R, Brune A. 2015. New mode of energy metabolism in the seventh order of methanogens as revealed by comparative genome analysis of “Candidatus Methanoplasma termitum.” *Appl. Environ. Microbiol.* **81**:1338–1352.

Lettinga G. 2010. Challenges of a feasible route towards sustainability in environmental protection. *Front. Environ. Sci. Eng. China* **4**:123–134.

Li Q, Yuwen C, Cheng X, Yang X, Chen R, Wang XC. 2018. Responses of microbial capacity and community on the performance of mesophilic co-digestion of food waste and waste activated sludge in a high-frequency feeding CSTR. *Bioresour. Technol.* **260**:85–94. http://www.sciencedirect.com/science/article/pii/S0960852418304498.

Li, Y., Leahy, S. C., Jeyanathan, J., Henderson, G., Cox, F., Altermann, E., … Attwood, G. T. (2016). The complete genome sequence of the methanogenic archaeon ISO4-H5 provides insights into the methylotrophic lifestyle of a ruminal representative of the Methanomassiliicoccales. *Standards in Genomic Sciences*, **11:**59.

Mulat DG, Ward AJ, Adamsen APS, Voigt NV, Nielsen JL, Feilberg A. 2014. Quantifying contribution of synthrophic acetate oxidation to methane production in thermophilic anaerobic reactors by membrane inlet mass spectrometry. *Environ. Sci. Technol.*

504 **48**:2505–2511.
505 Nordgård A, 2017. Microbial community analysis in developing biogas reactor technology
506 for Norwegian agriculture (Doctoral thesis). Retrieved from
507 https://brage.bibsys.no/xmlui/
508 Pelissari C, Guivernau M, Viñas M, de Souza SS, García J, Sezerino PH, Ávila C. 2017.
509 Unraveling the active microbial populations involved in nitrogen utilization in a vertical
510 subsurface flow constructed wetland treating urban wastewater. *Sci. Total Environ.*
511 **584**–**585**:642–650.
512 Penning H, Conrad R. 2007. Quantification of carbon flow from stable isotope fractionation
513 in rice field soils with different organic matter content. *Org. Geochem.* **38**:2058–2069.
514 Petersen SP, Ahring BK. 1991. Acetate Oxidation in A Thermophilic Anaerobic Sewage-
515 Sludge Digester - the Importance of Non-Aceticlastic Methanogenesis from Acetate.
516 *Fems Microbiol. Ecol.* **86**:149–157.
517 Prenafeta-Boldú FX, Rojo N, Gallastegui G, Guivernau M, Viñas M, Elías A. 2014. Role of
518 Thiobacillus thioparus in the biodegradation of carbon disulfide in a biofilter packed
519 with a recycled organic pelletized material. *Biodegradation* **25**:557–568.
520 Ruiz-Sánchez J, Campanaro S, Guivernau M, Fernández B, Prenafeta-Boldú FX. 2018.
521 Effect of ammonia on the active microbiome and metagenome from stable full-scale
522 digesters. *Bioresour. Technol.* **250**:513–522.
523 Schnürer A, Nordberg Å. 2008. Ammonia, a selective agent for methane production by
524 syntrophic acetate oxidation at mesophilic temperature. *Water Sci. Technol.* **57**:735–
525 740.
526 Schnürer A, Zellner G, Svensson BH. 1999. Mesophilic syntrophic acetate oxidation during
527 methane formation in biogas reactors. *FEMS Microbiol. Ecol.* **29**:249–261.
528 Sotres A, Díaz-Marcos J, Guivernau M, Illa J, Magrí A, Prenafeta-Boldú FX, Bonmatí A,

529 Viñas M. 2014. Microbial community dynamics in two-chambered microbial fuel cells:
530 Effect of different ion exchange membranes. *J. Chem. Technol. Biotechnol.*:n/a-n/a.
531 Sun L, Müller B, Westerholm M, Schnürer A. 2014. Syntrophic acetate oxidation in
532 industrial CSTR biogas digesters. *J. Biotechnol.* **171**:39–44.
533 Wang H, Fotidis IA, Angelidaki I. 2015. Ammonia effect on hydrogenotrophic methanogens
534 and syntrophic acetate-oxidizing bacteria. *FEMS Microbiol. Ecol.* **91**.
535 Westerholm M, Moestedt J, Schnürer A. 2016. Biogas production through syntrophic
536 acetate oxidation and deliberate operating strategies for improved digester
537 performance. *Appl. Energy*.
538 Whiticar MJ, Faber E. 1986. Methane oxidation in sediment and water column
539 environments-Isotope evidence. *Org. Geochem.* **10**:759–768.
540 Yamada T, Imachi H, Ohashi A, Harada H, Hanada S, Kamagata Y, Sekiguchi Y. 2007.
541 Bellilinea caldifistulae gen. nov., sp. nov and Longilinea arvoryzae gen. nov., sp. nov.,
542 strictly anaerobic, filamentous bacteria of the phylum Chloroflexi isolated from
543 methanogenic propionate-degrading consortia. *Int. J. Syst. Evol. Microbiol.* **57**:2299–
544 2306.
545 Yamada T, Sekiguchi Y, Hanada S, Imachi H, Ohashi A, Harada H, Kamagata Y. 2006.
546 Anaerolinea thermolimosa sp. nov., Levilinea saccharolytica gen. nov., sp. nov. and
547 Leptolinea tardivitalis gen. nov., sp. nov., novel filamentous anaerobes, and
548 description of the new classes Anaerolineae classis nov. and Caldilineae classis nov.
549 in the . *Int. J. Syst. Evol. Microbiol.* **56**:1331–1340.
550 Yenigün O, Demirel B. 2013. Ammonia inhibition in anaerobic digestion: A review. *Process*
551 *Biochem.* **48**:901–911.
552 Ziganshin AM, Ziganshina EE, Kleinsteuber S, Nikolausz M. 2016. Comparative analysis
553 of methanogenic communities in different laboratory-scale anaerobic digesters.

Archaea **2016**.

TABLE LEGENDS

Table 1. Results of the batch activity assays at different ammonia concentration in relation to the Specific rates of acetate consumption (*r*Ac) and methane production (*r*CH4), lag phase, methane yield and the apparent fractionation factor (αC). Depicted values correspond to the average and standard deviation of three independent replicates.

Table 2. Estimators of microbial species diversity/richness based on NGS of 16S rRNA genes and transcripts from the *Bacteria* and *Archaea* domains, obtained from the initial inoculum and after incubation during 11 and 17 days under increasing TAN concentrations. Predominant assigned genera (relative abundance > 5%) are also listed.

Table 3. Best match in BLAST searches (GenBank, NCBI, USA) on TAN-responding bacterial OTUs (see Figure 4). Only OTUs with a relative abundance in the original methanogenic biomass higher than 1% are listed.

LEGENDS TO FIGURES

Figure 1. Evolution of acetic acid (asterisks) and CH_4 (squares), both expressed as mg of COD equivalents, in batch reactors incubated at different TAN concentrations: (A) 1.0 gN-TAN L^{-1}; (B) 3.5 gN-TAN L^{-1}; and (C) 6.0 gN-TAN L^{-1}. The Gompertz equation (dashed line) was fitted to experimental methane yields (circles). Measured data are expressed as the average (sign) and the standard deviation (bars) of three independent batches.

Figure 2. Time-course quantitative PCR results from biomass samples of three independent batches incubated at 1.0, 3.5, and 6.0 gN-TAN L^{-1} (squares, circles, and triangles). The average (signs) and standard deviation (bars) of the ratio between number of transcripts and gene copies for the bacterial 16S rRNA (A) and the archaeal *mcrA* (B) has been depicted. Statistical significance in pairwise comparisons (n=3, p<0.05) in relation to the lowest ammonia exposure have been highlighted with an asterisk.

Figure 3. Relative abundance of bacterial (A) and archaeal (B) 16S rRNA genes and transcripts, expressed respectively at the order and genus phylogenetic level, in methanogenic batch reactors supplemented with increasing ammonia concentrations (1.0, 3.5, and 6.0 gN-TAN L^{-1}), and after different incubation times (0, 11, and 17 days). Each bar represents the average of two independent batches.

Figure 4. Ratio between the relative expression level of bacterial 16S rRNA transcripts obtained in batch methanogenic assays incubated at 3.5 gN-TAN L^{-1} (grey bar) and 6 gN-TAN L^{-1} (black bar), in relation to that at 1 gN-TAN L^{-1}. Assigned taxon and OTU number (in brackets) are indicated. Only the species with a relative abundance higher than 0.3% have been depicted.

Table 1

TAN ($gN\ L^{-1}$)	FAN [a] ($mgN\ L^{-1}$)	rAc [b] ($mgCOD\ gVSS^{-1}\ d^{-1}$)	rCH$_4$ [c] ($mgCOD\ gVSS^{-1}\ d^{-1}$)	Lag phase [c] (d)	Methane yield [c] ($mLCH_4\ gCOD^{-1}$)	αC [d]	Predominant methanogenic pathway [d]
1.0	114	16.80±0.42	13.61±0.25	6.37±0.15	238.41± 9.76	1.054±0.017	Acetotrophic
3.5	399	16.93±0.35	12.71±0.26*	6.28±0.13	245.63±13.54	1.077±0.001*	Hydrogenotrophic
6.0	683	9.10±0.35*	9.86±0.02*	10.17±0.10*	251.15± 2.21	1.080±0.000*	Exclusively hydrogenotrophic

[a] Calculated from the ammonium/ammonia chemical equilibrium in water at pH = 8 and T = 37°C.
[b] Measured empirically.
[c] From the mathematical fitting to the Gompertz equation (n=21, r^2>0.98).
[d] According to Conrad (2005).
* Statistically significant differences in relation to 1.0 gN-TAN L^{-1} (n=3, p<0.05).

Table 2

.

Parameter	Microbial group	Inoculum	1.0 g N-TAN L^{-1}		3.5 g N-TAN L^{-1}		6.0 g N-TAN L^{-1}	
			Genes	Transcripts	Genes	Transcripts	Genes	Transcripts
No. of reads	Bacteria	217,432	85,745	53,318	68,355	112,479	69,224	58,836
	Archaea	193,179	54,798	134,018	68,513	141,590	84,996	168,908
No. of OTUs [a]	Bacteria	4,720	3,241	2,032	3,110	3,514	3,105	2538
	Archaea	373	282	183	325	185	211	201
Coverage [b] (%)	Bacteria	99.42	99.90	99.87	99.85	99.92	99.88	99.85
	Archaea	99.97	99.89	99.96	99.92	99.96	99.92	99.97
Shannon (diversity)	Bacteria	4.05	3.89	4.30	4.02	4.64	3.92	4.62
	Archaea	2.72	2.39	1.48	2.37	1.52	2.13	1.70
Simpson (diversity)	Bacteria	8.76	7.66	24.03	8.21	24.37	7.31	26.68
	Archaea	8.02	6.73	2.80	5.71	3.11	4.93	3.34
Chao1 (richness) [c]	Bacteria	5,592 (64)	5,047 (127)	3,364 (116)	4,927 (126)	4,516 (77)	4,974 (130)	3,760 (99)
	Archaea	414 (14)	362 (25)	258 (28)	383 (17)	272 (33)	338 (44)	243 (16)
Predominant genera (% relative abundance)	Bacteria	*Longilinea* (36) *Clostridium* (10) *Bacteroides* (9) *Leptolinea* (7)	*Longilinea* (39) *Leptolinea* (11) *Clostridium* (9) *Bacteroides* (6)	*Alkaliphilus* (13) *Sphingobacterium* (11) *Leptolinea* (9) *Levilinea* (6) *Mariniphaga* (6) *Synergistes* (6) *Pseudomonas* (6)	*Longilinea* (38) *Clostridium* (9) *Bacteroides* (8) *Leptolinea* (6)	*Alkaliphilus* (17) *Sphingobacterium* (11) *Leptolinea* (6) *Pseudomonas* (6) *Mariniphaga* (5)	*Longilinea* (40) *Bacteroides* (10) *Clostridium* (9) *Synergistes* (5)	*Alkaliphilus* (17) *Leptolinea* (8) *Pseudomonas* (7) *Symbiobacterium* (6) *Levilineaca* (5) *Mariniphaga* (5)
	Archaea	*Methanoculleus* (31) *Methanobrevibacter* (26) *Methanosarcina* (20) *Methanosaeta* (10) *Nitrosocaldus* (7)	*Methanoculleus* (39) *Methanosarcina* (16) *Methanosaeta* (15) *Methanobrevibacter* (12) *Methanomassiliicoccus* (11)	*Methanosaeta* (48) *Methanoculleus* (40) *Methanomassiliicoccus* (7)	*Methanoculleus* (39) *Methanomassiliicoccus* (22) *Methanosarcina* (16) *Methanosaeta* (9) *Methanobrevibacter* (7)	*Methanosaeta* (40) *Methanoculleus* (47) *Methanomassiliicoccus* (9)	*Methanoculleus* (35) *Methanomassiliicoccus* (31) *Methanosarcina* (14) *Methanobrevibacter* (8)	*Methanoculleus* (45) *Methanomassiliicoccus* (36) *Methanosaeta* (10)

[a] Observed number of species based on operational taxonomic units (at 97% sequence homology cut-off).
[b] Good's estimator of coverage calculated as (1−(singletons/reads)) × 100.
[c] Estimated number of species average and standard deviation (between brackets).

Table 3

.

OTU nr	Identification [a]	Abundance (%)	Accession nr	H (%)	Source
1	*Longilinea*	30.31	JQ155218	99	Undefined full-scale anaerobic digester
2	*Leptolinea*	7.97	JQ104843	95	Undefined full-scale anaerobic digester
3	*Bacteroides*	7.67	GQ134121	99	Mesophilic anaerobic SBR treating swine waste (4.9 g N-TAN L^{-1})
6	*Levilinea saccharolytica*	1.15	EU407212	99	Household anaerobic digester
7	*Clostridium*	3.31	GQ995170	96	Mesophilic lab-scale anaerobic digester treating food industrial waste
12	*Acetivibrio*	1.45	GQ995163	99	Mesophilic lab-scale reactor treating food industrial waste
16	*Clostridium*	1.71	LN849648	99	Mesophilic lab-scale anaerobic digester reactor treating poultry manure
17	*Acholeplasma*	1.00	JN998160	99	Ammonium-stressed lab scale anaerobic digester
18	*Synergistes*	2.03	GQ134214	92	Mesophilic anaerobic SBR treating swine waste (1.0 g N-TAN L^{-1})
22	*Sterolibacterium denitrificans*	2.06	HM149064	92	Microbial fuel cell treating dairy wastewater
23	*Longilinea*	1.18	JQ104456	99	Undefined full-scale anaerobic digester
31	*Clostridium*	1.14	GQ136858	99	Mesophilic anaerobic SBR treating swine waste (5.2 g N-TAN L^{-1})
36	*Bacillus*	1.62	HQ183753	99	Undefined leachate sediment
2873	*Longilinea*	1.63	CU922827	98	Mesophilic anaerobic digester treating municipal wastewater sludge

[a] According to the GreenGenes database.

Figure 1

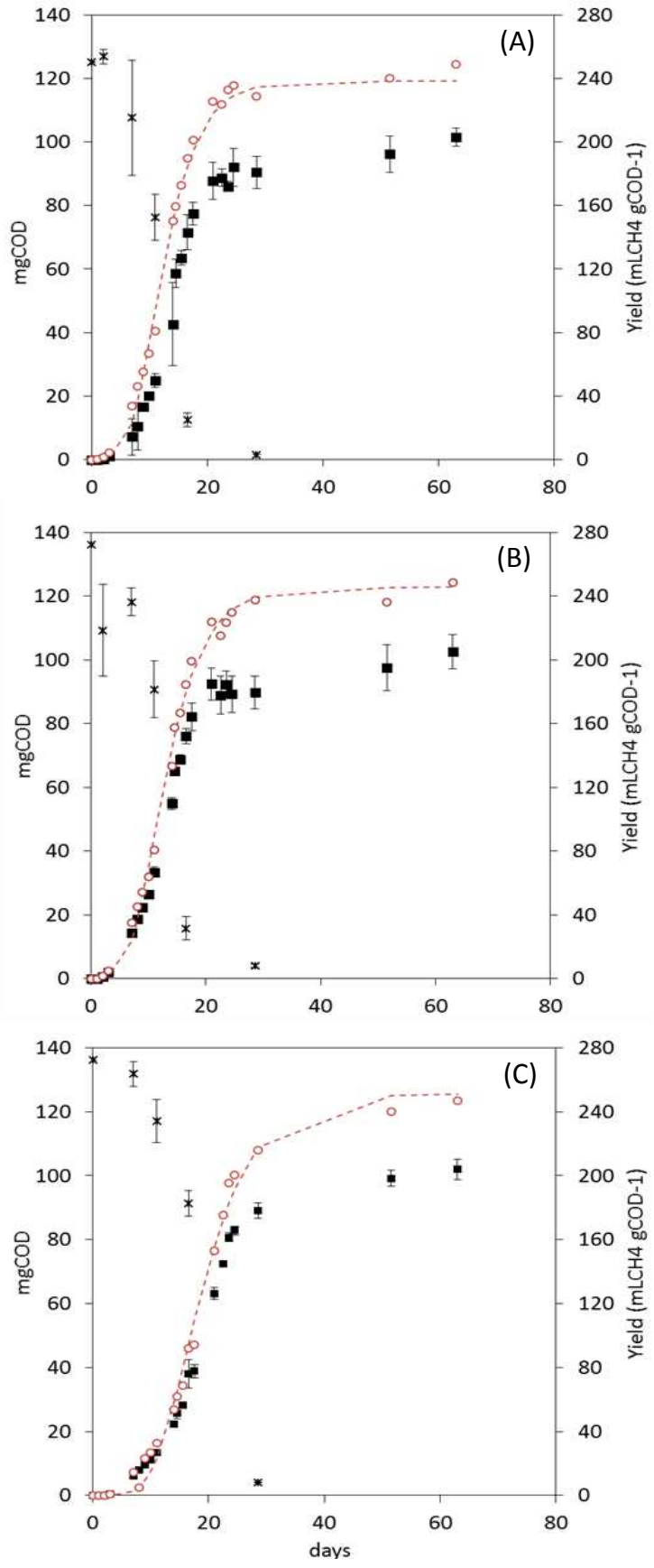
(A)
(B)
(C)
mgCOD
Yield (mLCH4 gCOD-1)
days
0
20
40
60
80
0
40
80
120
160
200
240
280
0
20
40
60
80
100
120
140

Figure 2

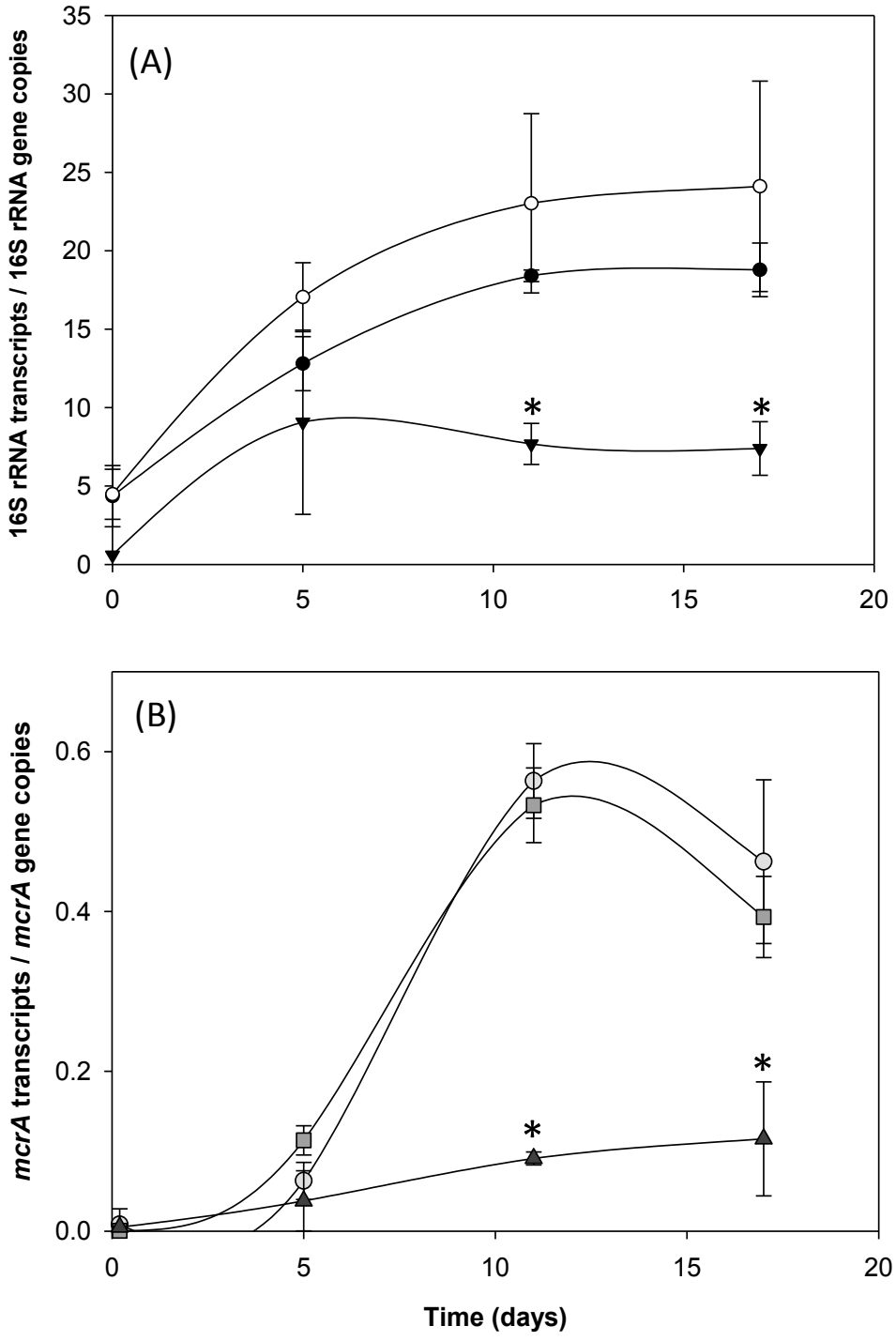
(A)
16S rRNA transcripts / 16S rRNA gene copies
35
30
25
20
15
10
5
0
0
5
10
15
20
*
*
(B)
mcrA transcripts / mcrA gene copies
0.6
0.4
0.2
0.0
0
5
10
15
20
*
*
Time (days)

Figure 3

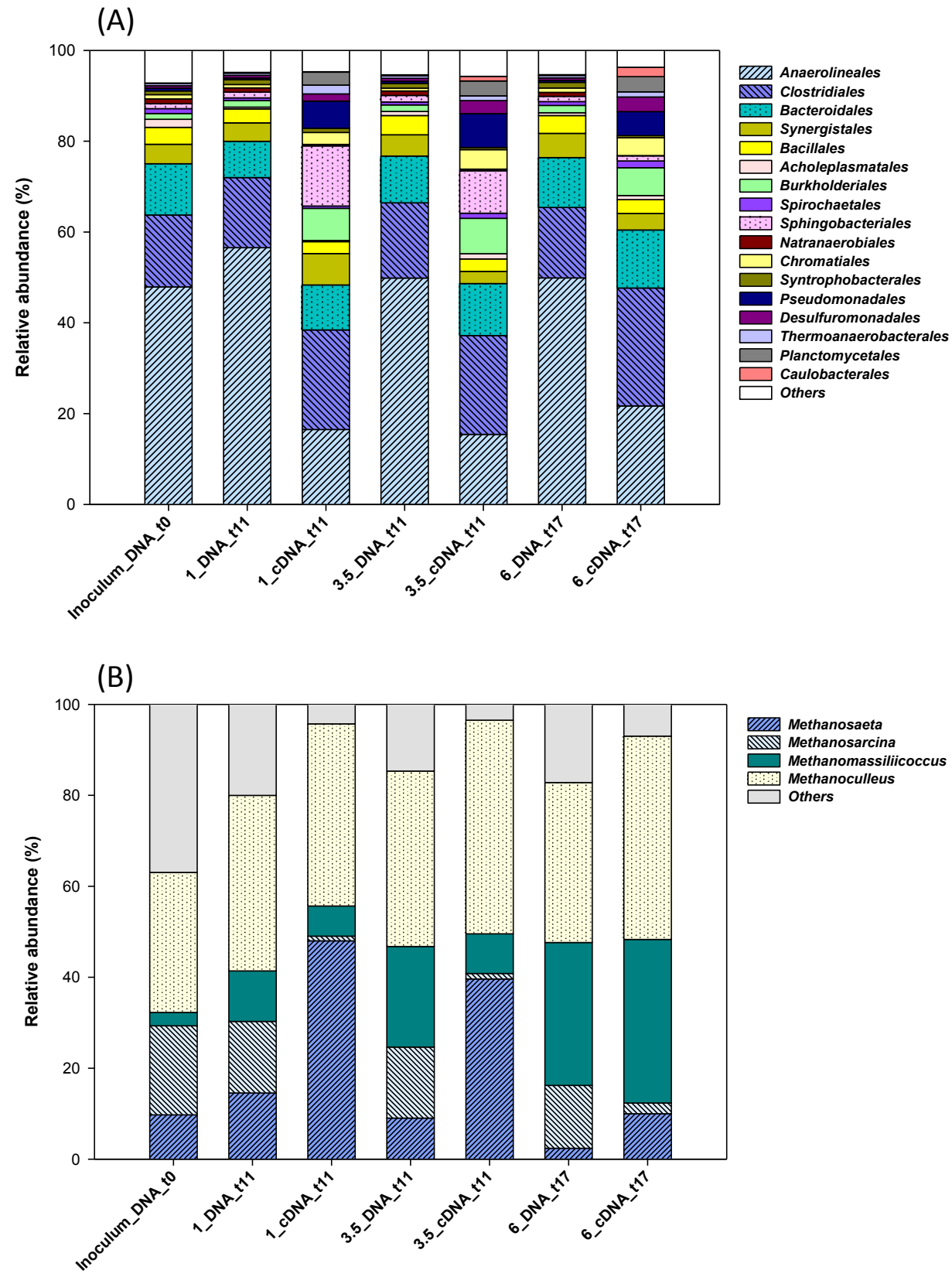
(A)
Relative abundance (%)
100
80
60
40
20
0
Inoculum_DNA_t0
1_DNA_t11
1_cDNA_t11
3.5_DNA_t11
3.5_cDNA_t11
6_DNA_t17
6_cDNA_t17
Anaerolineales
Clostridiales
Bacteroidales
Synergistales
Bacillales
Acholeplasmatales
Burkholderiales
Spirochaetales
Sphingobacteriales
Natranaerobiales
Chromatiales
Syntrophobacterales
Pseudomonadales
Desulfuromonadales
Thermoanaerobacterales
Planctomycetales
Caulobacterales
Others
(B)
Relative abundance (%)
100
80
60
40
20
0
Inoculum_DNA_t0
1_DNA_t11
1_cDNA_t11
3.5_DNA_t11
3.5_cDNA_t11
6_DNA_t17
6_cDNA_t17
Methanosaeta
Methanosarcina
Methanomassiliicoccus
Methanoculleus
Others

Figure 4

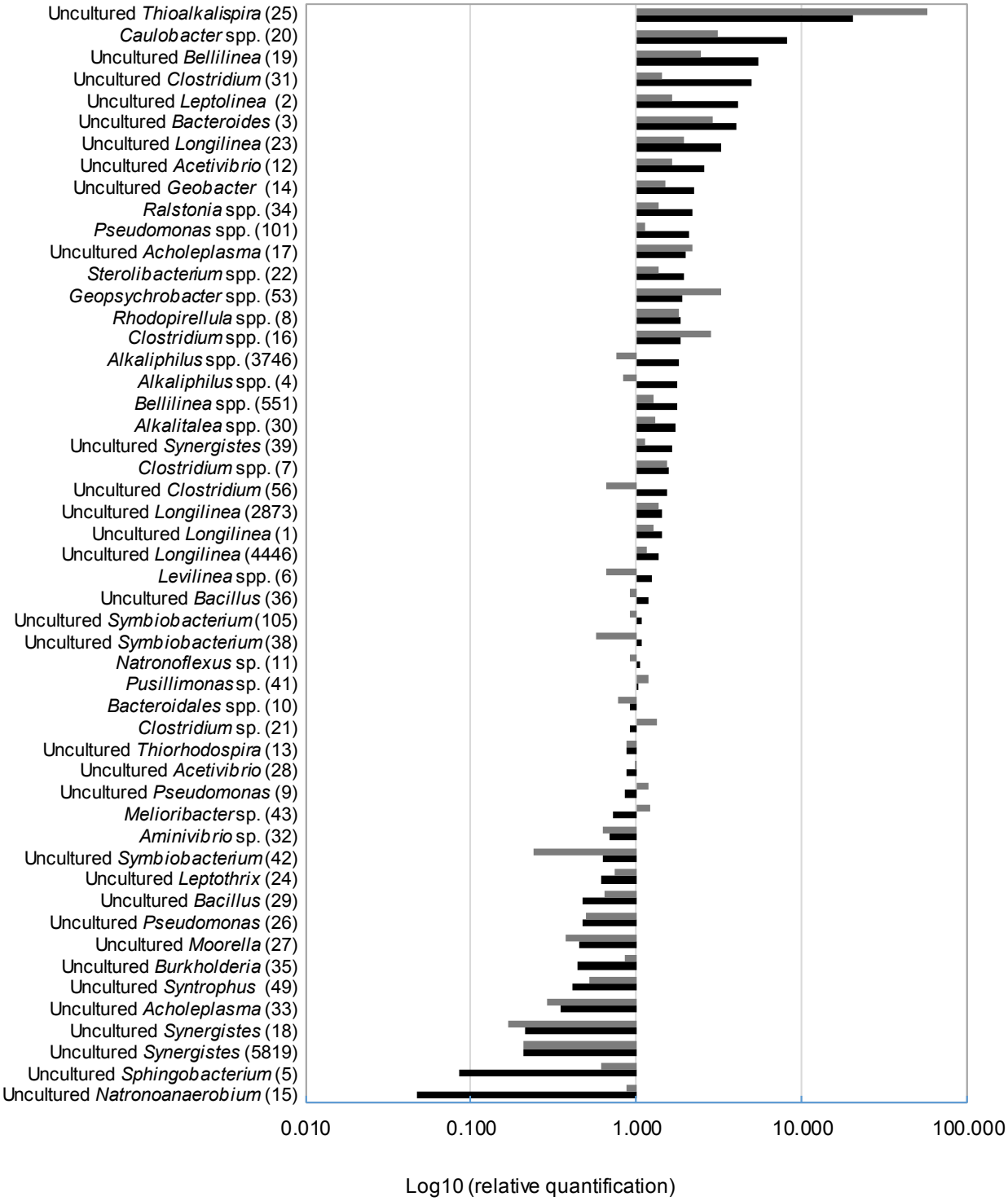
Uncultured *Thioalkalispira* (25)
Caulobacter spp. (20)
Uncultured *Bellilinea* (19)
Uncultured *Clostridium* (31)
Uncultured *Leptolinea* (2)
Uncultured *Bacteroides* (3)
Uncultured *Longilinea* (23)
Uncultured *Acetivibrio* (12)
Uncultured *Geobacter* (14)
Ralstonia spp. (34)
Pseudomonas spp. (101)
Uncultured *Acholeplasma* (17)
Sterolibacterium spp. (22)
Geopsychrobacter spp. (53)
Rhodopirellula spp. (8)
Clostridium spp. (16)
Alkaliphilus spp. (3746)
Alkaliphilus spp. (4)
Bellilinea spp. (551)
Alkalitalea spp. (30)
Uncultured *Synergistes* (39)
Clostridium spp. (7)
Uncultured *Clostridium* (56)
Uncultured *Longilinea* (2873)
Uncultured *Longilinea* (1)
Uncultured *Longilinea* (4446)
Levilinea spp. (6)
Uncultured *Bacillus* (36)
Uncultured *Symbiobacterium* (105)
Uncultured *Symbiobacterium* (38)
Natronoflexus sp. (11)
Pusillimonas sp. (41)
Bacteroidales spp. (10)
Clostridium sp. (21)
Uncultured *Thiorhodospira* (13)
Uncultured *Acetivibrio* (28)
Uncultured *Pseudomonas* (9)
Melioribacter sp. (43)
Aminivibrio sp. (32)
Uncultured *Symbiobacterium* (42)
Uncultured *Leptothrix* (24)
Uncultured *Bacillus* (29)
Uncultured *Pseudomonas* (26)
Uncultured *Moorella* (27)
Uncultured *Burkholderia* (35)
Uncultured *Syntrophus* (49)
Uncultured *Acholeplasma* (33)
Uncultured *Synergistes* (18)
Uncultured *Synergistes* (5819)
Uncultured *Sphingobacterium* (5)
Uncultured *Natronoanaerobium* (15)
0.010
0.100
1.000
10.000
100.000
Log10 (relative quantification)

Table1

Click here to download Table: table 1.docx

TAN ($gN\ L^{-1}$)	FAN [a] ($mgN\ L^{-1}$)	rAc [b] ($mgCOD\ gVSS^{-1}\ d^{-1}$)	rCH_4 [c] ($mgCOD\ gVSS^{-1}\ d^{-1}$)	Lag phase [c] (d)	Methane yield [c] ($mLCH_4\ gCOD^{-1}$)	αC [d]	Predominant methanogenic pathway [d]
1.0	114	16.80±0.42	13.61±0.25	6.37±0.15	238.41± 9.76	1.054±0.017	Acetotrophic
3.5	399	16.93±0.35	12.71±0.26*	6.28±0.13	245.63±13.54	1.077±0.001*	Hydrogenotrophic
6.0	683	9.10±0.35*	9.86±0.02*	10.17±0.10*	251.15± 2.21	1.080±0.000*	Exclusively hydrogenotrophic

[a] Calculated from the ammonium/ammonia chemical equilibrium in water at pH = 8 and T = 37°C.
[b] Measured empirically.
[c] From the mathematical fitting to the Gompertz equation (n=21, r^2>0.98).
[d] According to Conrad (2005).
* Statistically significant differences in relation to 1.0 gN-TAN L^{-1} (n=3, p<0.05).

Table 1

Table2
Click here to download Table: table 2.docx

Table 2

.

Parameter	Microbial group	Inoculum	1.0 g N-TAN L^{-1}		3.5 g N-TAN L^{-1}		6.0 g N-TAN L^{-1}	
			Genes	Transcripts	Genes	Transcripts	Genes	Transcripts
No. of reads	Bacteria	217,432	85,745	53,318	68,355	112,479	69,224	58,836
	Archaea	193,179	54,798	134,018	68,513	141,590	84,996	168,908
No. of OTU [a]	Bacteria	4,720	3,241	2,032	3,110	3,514	3,105	2538
	Archaea	373	282	183	325	185	211	201
Coverage [b] (%)	Bacteria	99.42	99.90	99.87	99.85	99.92	99.88	99.85
	Archaea	99.97	99.89	99.96	99.92	99.96	99.92	99.97
Shannon (diversity)	Bacteria	4.05	3.89	4.30	4.02	4.64	3.92	4.62
	Archaea	2.72	2.39	1.48	2.37	1.52	2.13	1.70
Simpson (diversity)	Bacteria	8.76	7.66	24.03	8.21	24.37	7.31	26.68
	Archaea	8.02	6.73	2.80	5.71	3.11	4.93	3.34
Chao1 (richness) [c]	Bacteria	5,592 (64)	5,047 (127)	3,364 (116)	4,927 (126)	4,516 (77)	4,974 (130)	3,760 (99)
	Archaea	414 (14)	362 (25)	258 (28)	383 (17)	272 (33)	338 (44)	243 (16)
Predominant genera (% relative abundance)	Bacteria	*Longilinea* (36) *Clostridium* (10) *Bacteroides* (9) *Leptolinea* (7)	*Longilinea* (39) *Leptolinea* (11) *Clostridium* (9) *Bacteroides* (6)	*Alkaliphilus* (13) *Sphingobacterium* (11) *Leptolinea* (9) *Levilinea* (6) *Mariniphaga* (6) *Synergistes* (6) *Pseudomonas* (6)	*Longilinea* (38) *Clostridium* (9) *Bacteroides* (8) *Leptolinea* (6)	*Alkaliphilus* (17) *Sphingobacterium* (11) *Leptolinea* (6) *Pseudomonas* (6) *Mariniphaga* (5)	*Longilinea* (40) *Bacteroides* (10) *Clostridium* (9) *Synergistes* (5)	*Alkaliphilus* (17) *Leptolinea* (8) *Pseudomonas* (7) *Symbiobacterium* (6) *Levilineaca* (5) *Mariniphaga* (5)
	Archaea	*Methanoculleus* (31) *Methanobrevibacter* (26) *Methanosarcina* (20) *Methanosaeta* (10) *Nitrosocaldus* (7)	*Methanoculleus* (39) *Methanosarcina* (16) *Methanosaeta* (15) *Methanobrevibacter* (12) *Methanomassiliicoccus* (11)	*Methanosaeta* (48) *Methanoculleus* (40) *Methanomassiliicoccus* (7)	*Methanoculleus* (39) *Methanomassiliicoccus* (22) *Methanosarcina* (16) *Methanosaeta* (9) *Methanobrevibacter* (7)	*Methanosaeta* (40) *Methanoculleus* (47) *Methanomassiliicoccus* (9)	*Methanoculleus* (35) *Methanomassiliicoccus* (31) *Methanosarcina* (14) *Methanobrevibacter* (8)	*Methanoculleus* (45) *Methanomassiliicoccu* *Methanosaeta* (10)

[a] Observed number of species based on operational taxonomic units (at 97% sequence homology cut-off).
[b] Good's estimator of coverage calculated as (1−(singletons/reads)) × 100.
[c] Estimated number of species average and standard deviation (between brackets).

Table3
Click here to download Table: table 3.docx

Table 3

.

OTU nr	Identification [a]	Abundance (%)	Accession nr	H (%)	Source
1	*Longilinea*	30.31	JQ155218	99	Undefined full-scale anaerobic digester
2	*Leptolinea*	7.97	JQ104843	95	Undefined full-scale anaerobic digester
3	*Bacteroides*	7.67	GQ134121	99	Mesophilic anaerobic SBR treating swine waste (4.9 g N-TAN L^{-1})
6	*Levilinea saccharolytica*	1.15	EU407212	99	Household anaerobic digester
7	*Clostridium*	3.31	GQ995170	96	Mesophilic lab-scale anaerobic digester treating food industrial waste
12	*Acetivibrio*	1.45	GQ995163	99	Mesophilic lab-scale reactor treating food industrial waste
16	*Clostridium*	1.71	LN849648	99	Mesophilic lab-scale anaerobic digester reactor treating poultry manure
17	*Acholeplasma*	1.00	JN998160	99	Ammonium-stressed lab scale anaerobic digester
18	*Synergistes*	2.03	GQ134214	92	Mesophilic anaerobic SBR treating swine waste (1.0 g N-TAN L^{-1})
22	*Sterolibacterium denitrificans*	2.06	HM149064	92	Microbial fuel cell treating dairy wastewater
23	*Longilinea*	1.18	JQ104456	99	Undefined full-scale anaerobic digester
31	*Clostridium*	1.14	GQ136858	99	Mesophilic anaerobic SBR treating swine waste (5.2 g N-TAN L^{-1})
36	*Bacillus*	1.62	HQ183753	99	Undefined leachate sediment
2873	*Longilinea*	1.63	CU922827	98	Mesophilic anaerobic digester treating municipal wastewater sludge

[a] According to the GreenGenes database.

Figure1

Click here to download Figure: Figure 1.docx

Figure 1

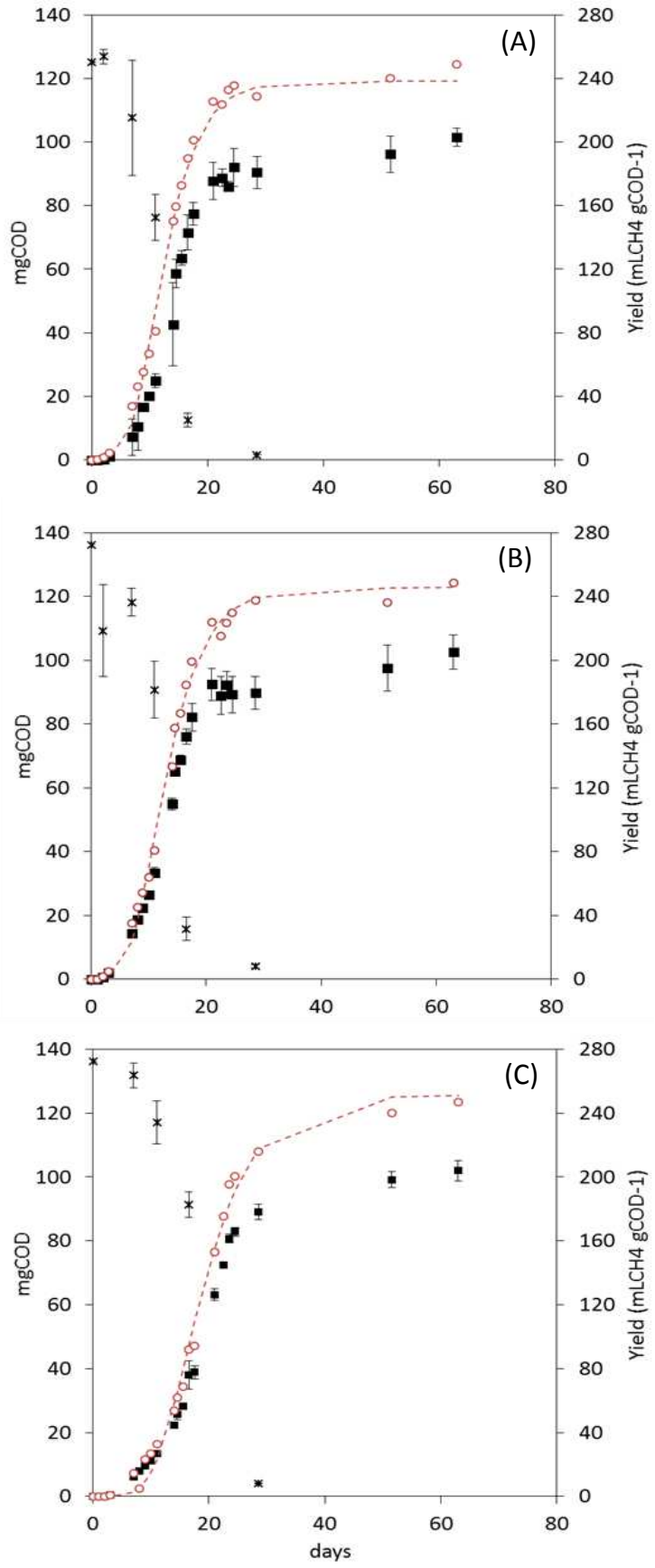

Figure2
Click here to download Figure: figure 2.docx

Figure 2

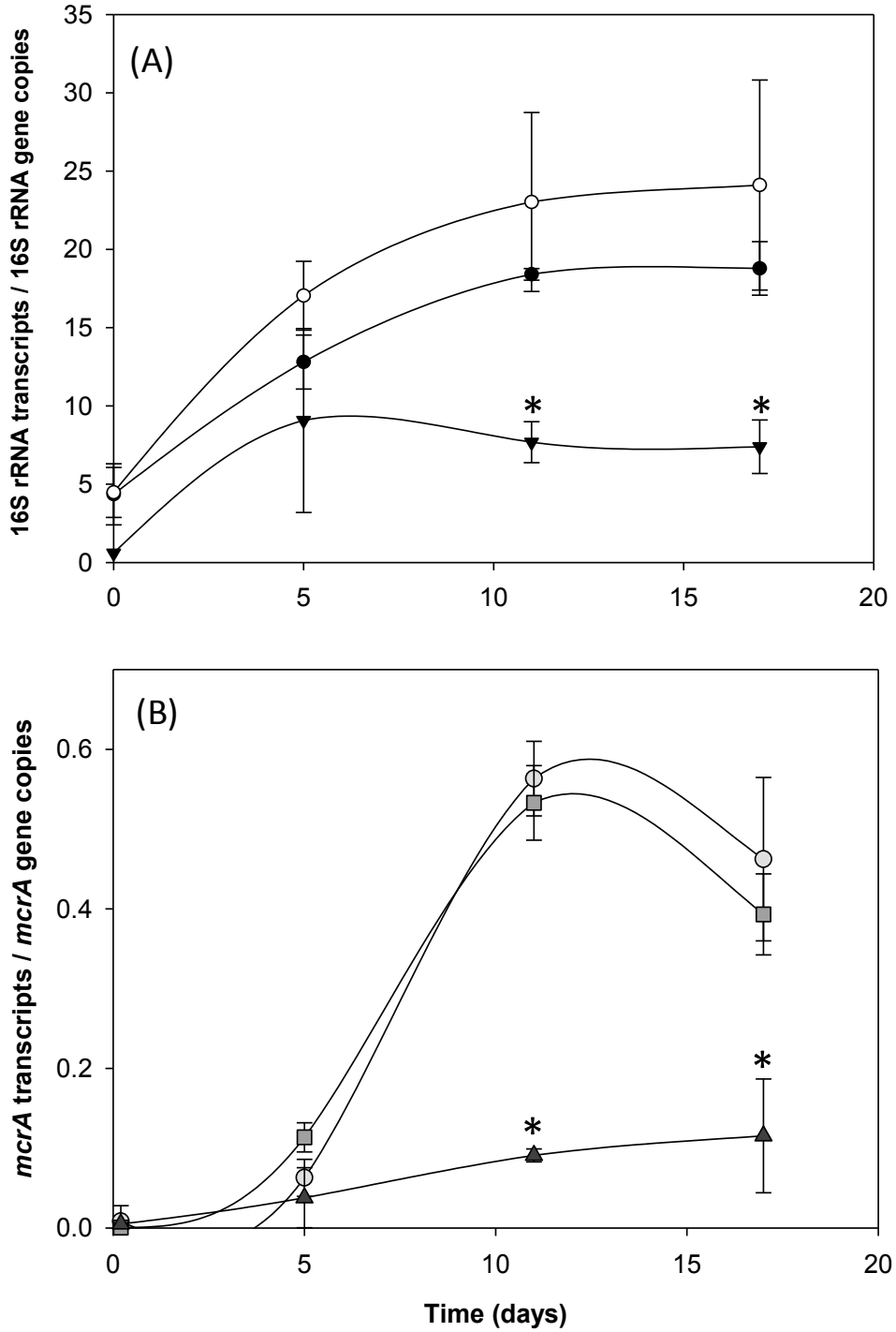

Figure3

Click here to download Figure: figure 3.docx

Figure 3

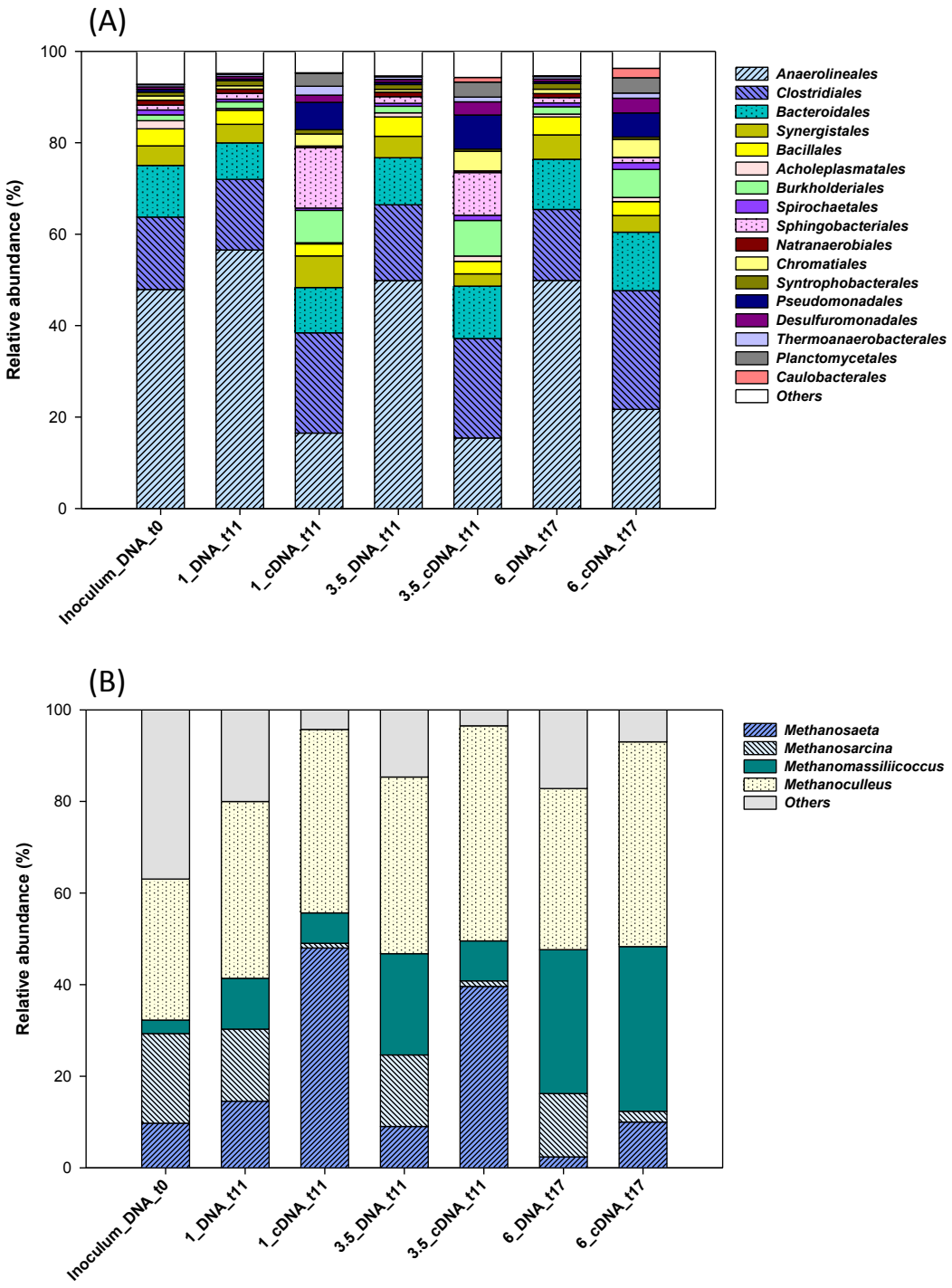

Figure4

Click here to download Figure: figure 4.docx

Figure 4